Neoarchean reworking of Mesoarchean and Paleoarchean crust (3.4~3.0 Ga) within the North China Craton: Constraints from zircon U-Pb geochronology and Lu-Hf isotopes from the basement of the Bohai Bay Basin

Fanchao Meng [1,2], Yulu Tian[1], Andrew C. Kerr[3], Qianjun Wang[4], Yong Chen[1,2], Yaoqi Zhou[1,2], Fei Yang[1]

1. School of Geosciences, China University of Petroleum (East China), Qingdao 266580, China

2.Key Laboratory of Deep Oil and Gas, China University of Petroleum (East China), Qingdao 266580, China

3. School of Earth and Environmental Sciences, Cardiff University, Cardiff, Wales CF10 3AT, United Kingdom

4. Exploration and Development Research Institute of Shengli Oilfield Company, SINOPEC, Dongying, Shandong Province, 257015, China

Abstract: The Bohai Bay Basin basement is composed mainly of Archean granitoid gneisses with minor supracrustal rocks and is the largest basin in the Eastern Block of the North China Craton. Due to a cover of Mesozoic and Cenozoic strata, little is known about the age and crustal evolution of this basement. In this study we report new zircon SHRIMP and LA-ICP-MS U-Pb and Lu-Hf isotope data for drill core samples, including TTGs (granodiorite, tonalite gneiss, trondhjemite gneiss), granites (monzogranite, syenogranite) and leptite, with the aim of revealing the Archean crustal evolutionary history of the Bohai Bay Basin basement. The U-Pb age of magmatic zircons from these granitoids reveals that basement rocks were mainly generated by two-stage events at ~3.1 Ga and ~2.5 Ga. The $\varepsilon_{Hf}(t)$ values of ~3.1 Ga magmatic zircons vary from +0.56 to +8.27, and their corresponding single-stage model ages range from 3.3 Ga to 3.0 Ga. The $\varepsilon_{Hf}(t)$ values of ~2.5 Ga magmatic zircons range from -12.87 to -0.07, their corresponding two-stage model ages range from 3.8 Ga to 2.9 Ga with most ages from 3.4 Ga to 3.0 Ga. The Hf isotopic characteristics show that the crustal growth of basement beneath Bohai Bay Basin occurred mainly between 3.4 and 3.0 Ga, different from crustal accretion ages of 2.9–2.7 Ga on the

periphery of the Bohai Bay Basin. However, both areas were reworked by the ~2.5 Ga tectono-thermal event. Integration of this new data from the basin basement with previous data, indicates that the Eastern Block of the North China Craton may have been formed by a mantle plume during the ~2.5 Ga period. The results from this study are significant in assessing the tectonic environment of the eastern basement in the North China Craton.

Key words: North China Craton; Bohai Bay Basin basement; Mesoarchean-Neoarchean; granitoid; Zircon U-Pb dating; Zircon Lu-Hf isotopes; Crustal reworking

1. Introduction

The North China Craton (NCC) is a general term used to refer to the Chinese part of the Sino-Korean Platform, covering most of North China, Inner Mongolia, Bohai Bay and the northern part of the Yellow Sea (Zhao et al., 2001a) (Fig.1a). The NCC is one of the oldest continental fragments with 3.8 Ga crustal rocks and detrital zircons up to ~4.1 Ga (Liu et al., 1992; Song et al., 1996). The Precambrian metamorphic basement of the NCC can be divided into the Western Block (WB) and Eastern Block (EB), which are separated by the Trans-North China Orogen (TNCO) (Zhao et al., 2005). Most Archean rocks in the NCC are exposed in the Eastern Block. U-Pb geochronology on magmatic zircon reveals that the EB underwent a significant number of tectono-magmatic events, between~3.8 Ga and ~1.8 Ga (Jahn et al., 2008; Wang et al., 2014; Wu et al., 2014; Xie et al., 2014). Events dated at 2.8–2.7 Ga and 2.6–2.5 Ga display evidence for the most significant tectono-thermal events and major periods of crustal growth (Zhu et al., 2013; Diwu et al., 2011; Geng et al., 2012; Sun et al., 2020). However, rocks older than 2.7 Ga in the NCC commonly underwent metamorphism and deformation at 2.6–2.5 Ga. Therefore, the major period of continental growth in the NCC could be 2.8–2.7 Ga, which is consistent with a peak in global crustal growth (Zhai and Bian, 2000). The 2.6–2.5 Ga rocks probably represent a special event of crustal growth and reworking in the NCC (Wan et al.,2012a).

Abundant 2.6–2.5 Ga TTGs (Trondhjemite-Tonalite-Granodiorites) have Hf-in-zircon and Nd whole-rock model ages that mostly range from 2.8 to 2.7 Ga with some at 2.6–2.5 Ga (Zhu et al., 2013; Zhai, 2014). It has been proposed that the 2.6–2.5 Ga TTGs or other magmatic

rocks were mostly formed by partial melting of 2.8–2.7 Ga rocks (Diwu et al., 2011; Geng et al., 2012; Wan et al., 2012a; Wu et al., 2016). Only some magmatic zircons in 2.6–2.5 Ga rocks yield negative zircon ε_{Hf} values and have Hf model ages greater than ~2.8 Ga (Zhai, 2014), indicating reworking of the Mesoarchean and Paleoarchean crustal rocks at 2.6~2.5 Ga. However, it is still unclear why the 2.7-2.8 Ga crust mainly remelted in this tectono-thermal event, and why there are few records of the Mesoarchean and Paleoarchean crustal rocks being melted at the same time?

The Bohai Bay Basin (BBB) is the largest basin in the EB of the NCC. However, the BBB basement is extensively covered by Mesoproterozoic and younger sedimentary sequences. Recently, some samples from drill holes were dated by U-Pb zircon, and Precambrian ages of ~2.5 Ga and ~3.0 Ga were obtained (Song et al., 2011; Wan et al., 2014b; Meng et al., 2017; Wang et al., 2019), proving the existence of Precambrian rocks beneath the BBB. Although Archean tectono-thermal events have been identified beneath the BBB, the lack of studies on the origin of Neoarchean rocks has limited our understanding of the tectonic setting of the late Neoarchean in the EB.

In this study, we report new zircon U-Pb age and Lu-Hf isotope data for Archean granitoids from drill holes that penetrated the BBB basement in the EB of the NCC. In combination with previous studies, the present study provides new constraints not only on the timing of magmatism but also on the crustal evolution beneath the BBB during the Archean. The results provide a new perspective on the tectonic setting of the EB on the NCC during 2.6-2.5 Ga.

2. Geological setting and samples

The NCC is composed of Eastern and Western blocks, separated by the Paleoproterozoic Trans-North China Orogen (Zhao et al., 2001a; Yang et al., 2008). The Western Block includes the Yinshan and Ordos blocks, separated by the Paleoproterozoic Khondalite Belt (Wang et al., 2011a; Yin et al., 2014). While the Eastern Block can be further subdivided into the Langrim and Longgang blocks separated by the Jiao-Liao-Ji Belt, which resulted from a series of rifting-subduction-collision events (Liu et al., 2020; Wang et al., 2020). The BBB is one of the largest basins in the Eastern Block of the NCC,

bordering the Yinshan-Yanshan orogenic belt in the north, the Taihang orogen uplift in the west, the Western Shandong uplift in the southeast, and the Jiaodong and Liaodong uplifts in the east (Fig.1b). The BBB consists of the Jizhong, Linqing, Huanghua, Jiyang, Bozhong and Liaohe depressions separated by uplifted older strata, including the XingNing, CangXian and ChengNing uplifts (Fig.1b).

Fig.1

Archean rocks (＞3.8Ga–~2.5Ga) are widespread around the BBB, including Western Shandong (WS), Eastern Hebei (EH), Western Liaoning (WL), Southern Liaoning (SL), Eastern Shandong (ES) (Zhao et al., 2005) (Fig.1a). The distribution of pre-Neoarchean (3.8 Ga–2.8 Ga) rocks is sporadic in WL, ES, and EH (Liu et al., 1992). Neoarchean rocks (~2.8–~2.5Ga) constitute most of the exposure of Archean basement around the BBB, including ES, WS, EH, WL and SL (Zhao et al., 2005; Wu et al., 2008; Wan et al., 2011; Zhai and Santosh, 2011; Wan et al., 2014a; Wu et al., 2014; Wang et al., 2015). In recent years, a few boreholes have revealed the existence of Precambrian basement beneath the BBB (Meng et al., 2017; Wang et al., 2019). However, little information about the early Precambrian is known from the basement of the BBB (Wan et al., 2014b), because of the covering Paleozoic to Cenozoic strata (Li et al., 2005).

In this study, samples were collected from drill cores at different depths in nine boreholes that penetrated the BBB basement. These boreholes are all located in the Chengdong uplift in the Jiyang depression in the BBB (Fig.1c). We analysed nine fresh samples, including six TTGs (massive granodiorite, Fig.2a-b; tonalitic gneiss, Fig.2c; tonalitic gneiss with migmatized felsic veins, Fig.2d; trondhjemitic gneiss, Fig.2e; trondhjemitic gneiss with migmatized felsic spots, Fig.2f), two granites (monzogranite, Fig.2g; syenogranite, Fig.2h) and one supracrustal rock (leptite, Fig.2i). The TTGs and granites were metamorphosed to gneisses, displaying blastic texture and directional structure, some of which experienced migmatization (Fig.2c, d, f). The TTG gneisses are composed of plagioclase (50–70%), quartz (20–30%), biotite (5–15%), and alkali feldspar (±5%) with accessory minerals of zircon, apatite and magnetite (Fig.3a-f). The granites are chiefly composed of plagioclase (15–30%), alkali feldspar (30–40%), quartz (20–35%), biotite (10–15%), and hornblende (5%), accompanied by zircon and magnetite, some

biotite and hornblende had been altered to chlorite and epidote. Plagioclase and alkalI feldspar are partially altered to sericite and calcite (Fig.3g-h). The supracrustal rock is composed mainly of quartz (75–80%), plagioclase (20–25%), and minor microcline (5%) with accessory minerals of zircon and magnetite (Fig.3i). Eight samples (except for the sample of the supracrustal rock) were analysed for major elements (Supplementary Table S1). Zircons in all nine samples were dated by U-Pb methods (Table1), and analysed for Lu-Hf isotopes.

Fig.2

Fig.3

Table1

3. Analytical methods

3.1. Major elements

Major element analyses were conducted at the Institute of Geology and Geophysical, Chinese Academy of Sciences (IGGCAS) in Beijing, China. X-ray fluorescence (XRF) was used to determine the major elements with the procedure reported by Guo et al.(2006). Estimated uncertainties range from 1% to 3% RSD for elements present at >1wt%, and 10% RSD for elements present at <1wt%. The GSR-3, a basalt reference material showed the values within the range of consensus values.

3.2. Zircon separation and CL imaging

Zircons from the drill cores were separated from 2–3 kg samples by standard heavy-liquid and magnetic techniques, followed by handpicking under a binocular microscope. The selected crystals were embedded in 25 mm epoxy disks and polished to approximately half their thickness. Zircon separation was conducted at the Beijing Createch Testing Technology Co., Ltd. (Beijing, China).

All zircon samples were examined using transmitted and reflected-light photomicrographs and CL image analysis to reveal their internal structures prior to U–Pb dating. CL imaging was performed with a scanning electron microscope (JSM 6150.cl) and detector (Gatan MiniCL) with a voltage of 10 kv. CL images of samples CHG14-2, CHG16-2, CHG19-3, CH96-1, and

CHG7-1 were obtained at the Institute of Geology, Chinese Academy of Geological Sciences (Beijing, China), and other samples (samples CHG12-2, CHX911-1, CHX912-3, and CH917-3) were obtained at Beijing Createch Testing Technology Co., Ltd. (Beijing, China).

3.3. SHRIMP zircon dating

Single-zircon U-Pb dating was conducted using SHRIMP II at the Institute of Geology, Chinese Academy of Geological Sciences (Beijing, China). U-Th-Pb isotopic ratios were corrected for instrumental interelement fractionation using zircon standard TEM with $^{206}Pb/^{238}U$ = 0.0668 at 417 Ma. U, Th and Pb absolute abundances were calibrated using the zircon standard SL13 (572 Ma) with U = 238 ppm and Th = 18 ppm (Black et al., 2004). The two zircon standards were provided by Australian National University. Data were processed using the Ludwig SQUID 1.0 and ISOPLOT 4.15 programs. Measured compositions were corrected for common Pb using nonradiogenic ^{204}Pb. The analysis conditions included an approximately 15 nA, 10 kV O^{2-} beam with a spot size of 30 μm in diameter. A single spot on each zircon grain was analysed for approximately 20 min. A zircon U-Pb international standard was analysed for every three U-Pb single-spot analyses of the samples to monitor the analytical accuracy, external precision and instrumental drift. The mass resolution used for measuring Pb/Pb and Pb/U isotopic ratios was approximately 5,000. The SHRIMP U–Pb data are presented as a concordia plot (Fig. 7a-e) and in Supplementary Table S2. The uncertainties of the individual analyses are shown at the 2σ level. Magmatic crystallization ages, indicated by the mean $^{206}Pb/^{238}U$ age, are reported with a 95% confidence interval (2σ).

3.4. LA-ICP-MS zircon dating and Lu-Hf isotopic analysis

U-Pb analyses were conducted by LA-ICP-MS at Beijing GeoAnalysis Co., Ltd. Laser sampling was performed using an ESI NWR 193 nm laser ablation system. An AnlyitikJena PQMS Elite ICP-MS instrument was used to acquire ion-signal intensities. Helium was used as a carrier gas. Argon was used as the make-up gas and mixed with the carrier gas via a T-connector before entering the ICP. Each analysis incorporated a background acquisition of approximately 15–20 s (gas blank) followed by 45 s data acquisition from the sample. Off-line raw data selection, integration of background and analyte signals, time-drift correction and

quantitative calibration for U-Pb dating were carried out by ICPMSDataCal (Liu et al., 2010). Zircon GJ-1 was used as an external standard for U-Pb dating and was analysed twice every 5–10 analyses. Time-dependent drifts of U-Th-Pb isotope ratios were corrected using linear interpolation (with time) for every 5–10 analyses according to the variations in GJ-1 (i.e., 2 zircon GJ-1 + 5–10 samples + 2 zircon GJ-1) (Liu et al., 2010). Uncertainty of preferred values for the external standard GJ-1 was propagated to the ultimate results of the samples. In all analysed zircon grains, a common Pb correction was not necessary due to the low signal of common ^{204}Pb and high $^{206}Pb/^{204}Pb$. U, Th and Pb concentrations were calibrated by NIST 610. Concordia diagrams and weighted mean calculations were made using Isoplot/Ex_ver4.15. The zircon Plesovice was dated as an unknown sample and yielded a weighted mean $^{206}Pb/^{238}U$ age of 337.5 ± 1.5 Ma (2SD, n = 11), which is in good agreement with the recommended $^{206}Pb/^{238}U$ age of 337.13 ± 0.37 Ma (2SD) (Sláma et al., 2008). The LA-ICP-MS zircon U–Pb age data are listed in Supplementary Table S3.

The zircon Lu-Hf isotopic analyses were carried out at Beijing GeoAnalysis Co., Ltd. (Beijing, China) with a RESO 193 nm laser ablation system and a Neptune Plus MC-ICP-MS. During the experiment, helium was used as the carrier gas for the ablation material, and the laser beam's spot diameter was 40 μm. The internationally accepted standard zircon Plešovice was used as the reference material in this test (Sláma et al., 2008). Detailed analytical procedures are described in Wu et al. (2006). The $^{176}Hf/^{177}Hf$ value of the standard zircon Plešovice acquired during these analyses was 0.282480±0.000016 (2σ) (Sláma et al., 2008) within the error range. In the calculation of the $\varepsilon_{Hf}(t)$ values, the $^{176}Hf/^{177}Hf$ and $^{176}Lu/^{177}Hf$ ratios of present-day chondrite and the depleted mantle used were (0.0332, 0.282772) and (0.0384, 0.28325), respectively (Griffin et al., 2000). The two-stage Hf model ages (T_{DM2}) were calculated by adopting $^{176}Lu/^{177}Hf = 0.015$ for average continental crust (Griffin et al., 2000).

4. Results

4.1. Major element composition

Among the eight samples analysed in this paper, the six TTGs (CHG14-2，CHG16-2, CHG19-3, CHG12-2，CHX911-1 and CHX912-3) show high SiO_2 contents (63.1 wt.%-73.5 wt.%), a wide range of K_2O concentrations (0.6 wt.%-3.4 wt.%) and Na_2O/K_2O ratios (1.1 -7.3.

The two samples (CH96-1 and CHG7-1) from the granites display SiO_2 contents of 65.0 wt.%-70.9 wt.%, MgO contents of 1.0 wt.%-2.6 wt.%, with a low Na_2O/K_2O ratios (~0.8). According to the An-Ab-Or diagram, CHG19-3 and CHG16-2 fall within tonalites, CHG14-2 and CHG12-2 belong to granodiorites, CHX912-3 and CHX911-1 are trondhjemites, CH96-1 and CHG7-1 are indeed granites samples (Fig.4).

Fig.4

4.2. Zircon U-Pb ages

4.2.1. TTGs

Three samples (CHG14-2，CHG16-2 and CHG19-3) of the TTGs were dated by zircon SHRIMP U-Pb method, and other three samples (CHG12-2，CHX911-1 and CHX912-3)were dated by LA-ICP-MS U-Pb method.

Zircons from sample CHG14-2 (a granodiorite) exhibit euhedral crystal shapes and oscillatory zoning, with most having a length to width ratio of 2:1. Some crystals show slight partial recrystallization rims (Fig.5A). Fifteen analyses from fifteen zircons on domains with oscillatory zoning have Th/U ratios of 0.03–0.60 (excluding spot 8, with Th/U ratios of 1.58). If the most discordant analysis (spot 11) is excluded, the remaining 14 analyses yield a discordia line with an upper intercept age of 3131±23 Ma (MSWD=0.9), in which the most concordant analysis has a $^{207}Pb/^{206}Pb$ age of 3119±7.7 Ma (spot 12 with a Th/U ratio of 0.37), nearly the same age as the upper intercept age (Fig. 7a). Spot 11 yielded a $^{207}Pb/^{206}Pb$ age of 2923±6.9 Ma. Consequently, 3131±23 Ma is the crystallization age of the granodiorite.

Zircons from sample CHG16-2 (a tonalite gneiss) display euhedral, long prismatic shapes with lengths and length to width ratios of 100–220 μm and 1.5:1–3:1, respectively. Most zircons have oscillatory zones. The Th/U ratios of zircons are 0.04–0.40 (mostly >0.1), which are typical features of zircons crystallized from a melt (Fig. 5B). Seventeen analyses were conducted on sixteen zircons from the sample. The data are discordant and show slight scatter. Except for four spots (spots 1, 4, 9, and 17), thirteen analyses defined a discordia line with an upper age of 2598±31 Ma (MSWD=1.6), consistent with the most concordant 11 analyses, which have an apparent $^{207}Pb/^{206}Pb$ age of 2601±18 Ma. Consequently, we consider 2598±31 Ma as the emplacement time of the tonalite.

Fig.5

Most zircons from sample CHG19-3 (a tonalite gneiss) are subhedral to euhedral and stubby to long prismatic in shape with lengths of 120 – 225 μm, widths of 60–120 μm and length to width ratios of 1:1–4:1, and have pronounced oscillatory zoning in CL images (Fig. 5C). Seventeen U-Pb analyses were performed on fifteen zircons. Seventeen grains had variable uranium and thorium concentrations of 205–11645 ppm and 88–3379 ppm. Zircons had high Th/U ratios of 0.15–1.02, indicating magmatic zircons. Seventeen analyses approximately constitute a line with an upper intercept age of 2533±27 Ma (MSWD=3.2) (Fig. 7c), which may well be the emplacement age of the tonalite.

Zircons from CHG12-2 sample (a granodiorite) are euhedral and stubby with long axes ranging from 100 to 200 μm in length. In CL images, zircons have well-developed concentric, oscillatory zoning with strong luminescence. Forty-four U-Pb analyses were performed on forty zircons (Fig. 6A). They have U contents of 26–22185 ppm, Th contents of 48–6635 ppm, and high Th/U ratios of 0.03–0.62 (mostly >0.1). The internal structures and Th/U ratios indicate that they are all typical magmatic zircons. Most analysed spots, excluding spot 15, are essentially discordant (Fig. 7f), suggesting that they experienced variable Pb loss due to subsequent tectono-thermal or metamorphic events. Thirty-six spots were selected to confirm the formation age of the granodiorite. These fit a discordia line with an upper concordia intercept age of 3123±23 Ma (MSWD=1.2), consistent with only one concordant age of 3127±50 Ma (Fig. 7f). The age of 3123±23 Ma is taken as the crystallization age of the granodiorite. The remaining eight analyses, which are highly discordant with apparent $^{207}Pb/^{206}Pb$ ages of 1603–2253Ma, are possibly related to a high degree of Pb loss.

Fig.6

Zircons from sample CHX911-1 (a trondhjemite gneiss) show similar characteristics to those of sample CHG12-2, except the zircon grains are smaller than those in CHG12-2. Some zircons have corroded magmatic cores (Fig.6B). Thirty-three zircon grains were analysed for U-Pb isotopes on thirty-three spots. Among them, spot 1 was analysed on a magmatic core with a Th/U ratio of 0.53 and an apparent $^{207}Pb/^{206}Pb$ age of 2987±75 Ma, and represents an old inherited zircon grain, although it was not on a concordant line. The remaining thirty-two analyses can be fitted on a regression line with an upper intercept age of 2500±23 Ma (MSWD=2.3) (Fig. 7f), consistent with a weighted mean $^{207}Pb/^{206}Pb$ age of 2507 Ma calculated

by the three concordant analyses. An age of 2500±23 Ma is taken as an estimate of the crystallization age of the trondhjemite.

Zircons from sample CHX912-3 (a trondhjemite gneiss) show similar size, length, length to width ratio and oscillatory zoning to those of sample CHX911-1 (Fig.6C). Among the twenty-one analyses of twenty-one zircon grains, the oldest age obtained was 2949±39 Ma (spot 10), but with high discordance and distance from the concordant line. The most concordant spot 2, has an apparent $^{207}Pb/^{206}Pb$ age of 2440±55 Ma with a Th/U ratio of 1.05 and oscillatory zoning in the CL image (Fig.6C). Together with two analyses, twenty spots define a discordia line with an upper intercept age of 2454±48 Ma (MSWD=0.5) (Fig.7h). Therefore, we interpret 2453±48 Ma as the emplacement time of the trondhjemite.

4.2.2. Granites

Two samples (CH96-1 and CHG7-1) from the granites were dated by the zircon SHRIMP U-Pb method.

Zircons obtained from sample CH96-1 (a monzogranite) are euhedral in shape with long axes ranging between 200 and 300 μm in length and length to width ratios of 3:2-3:1. In CL images, many zircon crystals contain internal relict zircons, showing core-rim structures. Both cores and rims have oscillatory zoning, and in some cases, it was difficult to distinguish rims from the cores (Fig.6D). Seventeen analyses were obtained from 14 zircon grains. The oldest age is from the core of a core-rim structure zircon (Fig.6D) with a $^{207}Pb/^{206}Pb$ concordant age of 3038±7 Ma and a Th/U ratio of 0.25, representing an inherited old zircon grain. The data from 5 analyses are discordant and show scatter, which makes an age determination difficult, although they show $^{207}Pb/^{206}Pb$ ages varying between 2663 Ma and 2849 Ma. The remaining eleven analyses with Th/U ratios of 0.08–1.22 yielded a discordia line with an upper intercept age of 2496±34 Ma (Fig.7d), which is taken as the best estimate of the crystallization age of the granite.

Zircons from sample CHG7-1 (a syenogranite) show similar features to those of sample CH96-1, except that they are slightly smaller (Fig.6E). Twelve analyses were carried out on nine zircons, in which three zircons have core and rim ages. They yielded U contents of 160–7702 ppm, Th contents of 89–351, and Th/U ratios of 0.15–0.81 (except spot 12, 1.09). Spot

12, with a Th/U ratio of 1.09, which was very different from other analyses, has an apparent $^{207}Pb/^{206}Pb$ age of 2303±27 Ma, reflecting different Pb loss from the other samples. The remaining eleven analyses constitute a good discordia line with an upper intercept age of 2503±24 Ma (MSWD=2.7) (Fig.7e), identical to the weighted mean age of 2476±15 Ma (MSWD=4.8). Consequently, 2503±24 Ma represents the crystallization age of the granite.

4.2.3. Supracrustal rocks

Zircons from sample CH917-3 (a leptite) show variable sizes, with most of them being long and up to 150 μm and with length to width ratios of 2:1-1:1 (Fig.6D). Forty-two analyses on 42 grains were obtained from the sample. Two groups of zircons were identified. The first group contains euhedral crystals with a long prismatic morphology and long axes ranging between 50 and 115 μm in length. They show clear oscillatory zoning with dark CL luminosity. Twenty-nine analyses yielded a discordia line with an upper intercept age of 2486±21 Ma (MSWD=2.3), identical to the weighted mean of a concordant age of 2481±20 Ma. Another group of zircons has oval shapes with lengths and length to width ratios ranging from 50 to 1100 μm and from 1.5:1 to 1:1, respectively. In CL images, they show weak oscillatory zoning and are generally surrounded by irregular rims. Thirteen analyses constitute a good discordia line with an upper intercept age of 3081±19 Ma (MSWD=0.3) (Fig.7i), consistent with the weighted mean of a concordant age of 3078±24 Ma. We therefore interpret 2486±21 Ma and 3081±19 Ma as the source ages of the supracrustal rocks.

Fig.7

4.3 Zircon Lu-Hf isotopes

Zircon Lu-Hf isotope analyses were conducted on the same domains as those of the previous U-Pb dating. The zircon Lu-Hf isotope results are listed in Supplementary Table S4. Zircon $\varepsilon_{Hf}(t)$ values were calculated at the crystallization age of each sample. For detrital zircons with ages of 3081±19 Ma and 2486±21 Ma from sample CH917-3, $\varepsilon_{Hf}(t)$ values were calculated at their apparent $^{207}Pb/^{206}Pb$ ages. The $\varepsilon_{Hf}(t)$ values and the distribution patterns of zircon Hf model ages (T_{DM}) are presented in Fig. 8 and Fig. 9.

Fig.8

Fig.9

4.3.1 TTGs

Six samples (CHG14-2, CHG16-2, CHG19-3, CHX911-1, CHX912-3, and CHG12-2) from the TTGs were analysed for zircon Lu-Hf isotopes.

Fifteen Lu-Hf analyses were performed on zircons from sample CHG14-2 (a granodiorite). Except for one analysis (spot 11) with high discordances of $^{207}Pb/^{206}Pb$ ages, fourteen Lu-Hf analyses yielded $\varepsilon_{Hf}(t)$ values of 1.19-5.56 with a weighted mean of 3.02±0.67 and T_{DM1} ages ranging from 3143 to 3306 Ma with a weighted mean of 3240±25 Ma.

Fourteen Lu-Hf analyses were made on zircons from sample CHG16-2 (a tonalite gneiss). Except for two analyses with high discordances of $^{207}Pb/^{206}Pb$ ages (spots 1 and 9), twelve Lu-Hf analyses yielded $\varepsilon_{Hf}(t)$ values of -11.37~-1.06 with a weighted mean of -6.2±1.8, and T_{DM2} ages ranging from 3761 to 3139 Ma with a weighted mean of 3447±110 Ma.

Seventeen Lu-Hf analyses on zircons from sample CHG19-3 (a tonalite gneiss) yielded $\varepsilon_{Hf}(t)$ values of -3.60~-0.49 (except spot 17, $\varepsilon_{Hf}(t)$=-0.07) with a weighted mean of -1.47±0.5 and T_{DM2} ages ranging from 3242 to 3053 Ma with a weight mean of 3112±30 Ma (except 17, T_{DM1}=2843 Ma).

Twenty-eight Lu-Hf analyses were performed on zircons from sample CHX911-1 (a trondhjemite gneiss). Except for one analysis with high discordances of $^{207}Pb/^{206}Pb$ ages, twenty-seven Lu-Hf analyses yielded $\varepsilon_{Hf}(t)$ values of -12.87 ~ -1.05 and T_{DM2} ages of 3777 ~ 3062 Ma.

Twenty-one Lu-Hf analyses were made on zircons from sample CHX912-3 (a trondhjemite gneiss). Except for one analysis with high discordances of $^{207}Pb/^{206}Pb$ ages, twenty Lu-Hf analyses yielded $\varepsilon_{Hf}(t)$ values of -11.36 ~ -2.93 with a weighted mean of -6.1±1.0 and T_{DM2} ages of 3650 ~ 3140 Ma with a weighted mean of 3333±61 Ma.

Forty-four Lu-Hf analyses were performed on zircons from sample CHG12-2 (a granodiorite). Except for eight analyses with high discordances of $^{207}Pb/^{206}Pb$ ages, thirty-six Lu-Hf analyses yielded $\varepsilon_{Hf}(t)$ values of +0.56 ~ +8.27 (except for spot 24, $\varepsilon_{Hf}(t)$=-1.49) with a weighted mean of 3.45±0.63 and T_{DM1} ages of 3329 ~ 3032 Ma with a weighted mean of 3211±22 Ma. (spot 24, T_{DM2}=3568±45 Ma).

4.3.2 Granites

Sixteen Lu-Hf analyses were performed on zircons from sample CH96-1 (a monzogranite). Nine analyses with a concordant age of 3038±7 Ma yield a $\varepsilon_{Hf}(t)$ value of -6.5±-0.64 and a T_{DM2} age of 3389±39 Ma. The remaining seven Lu-Hf analyses yield $\varepsilon_{Hf}(t)$ values of -12.0 ~ -2.28 with a weighted mean of -6.7±3.6 and T_{DM2} ages of 3722 ~ 3133 Ma with a weighted mean of 3418±140 Ma.

Twelve Lu-Hf analyses were made on zircons from sample CHG7-1 (a syenogranite). Except for one analysis with high discordances of $^{207}Pb/^{206}Pb$ ages (spot 12), eleven Lu-Hf analyses yielded $\varepsilon_{Hf}(t)$ values of -4.80 ~ -0.67 with a weighted mean of -2.23±0.87 and T_{DM2} ages of 3291 ~ 3041 Ma with a weighted mean of 3136±53 Ma.

4.3.3 Supracrustal rocks

Thirty-four Lu-Hf analyses were performed on zircons from sample CH917-3 (a leptite). The thirty-four Lu-Hf analyses comprise two groups. The first group (twenty-five analyses) with an upper intercept age of 2486±21 Ma yielded $\varepsilon_{Hf}(t)$ values of -11.54~0.83 and T_{DM2} ages of 3686 ~ 2937 Ma. The second group with an upper intercept age of 3081±19 Ma yielded $\varepsilon_{Hf}(t)$ values of +12.67 ~ +1.00 (except spot 39, -7.25) and the T_{DM1} ages of 3269 ~ 2809 Ma (except for spot 39, T_{DM2}=3522±46 Ma).

5 Discussion

5.1 Magmatism events of the BBB basement

Available zircon U-Pb data for the early Precambrian rocks from drill holes into the basement beneath the BBB are summarized in Table 2. In this study, magmatic zircon U-Pb data gave crystallization ages of ~3.1 Ga and 2.60–2.45 Ga for the protolith magmas of TTGs, granites and supracrustal rocks, in good agreement with previous zircon U-Pb ages of ~3.1 Ga and 2.6–2.5 Ga, respectively, obtained for different lithologies from drill holes within different depressions in the basement of the BBB (Song et al., 2011; Wan et al., 2014b; Wang et al., 2019). As shown in Table 2, in general, TTG magmatism, including granodiorite, tonalite and trondhjemite rocks, occurred during 3.16–3.12 Ga and 2.60–2.45 Ga, respectively. The diorite and granites were almost simultaneously emplaced at ~2.5 Ga. For the supracrustal rock (sample CH917-3), we obtained two magmatic ages of 2486±21 Ma and 3081±19 Ma, which

392 are consistent with previous magmatic zircon U-Pb ages of ~3166 Ma and 2.35–2.54 Ga from
393 the Jidong and Bozhong depressions (Wan et al., 2014b; Wang et al., 2019), respectively.
394 However, some magmatic zircons from supracrustal rocks in the Liaohe depression in the BBB
395 have an age of approximately 2600 Ma (Song et al., 2011). These different ages obtained from
396 the supracrustal rocks in the basement of the BBB suggest that the detrital zircons in the
397 supracrustal rocks come from various sources. The ~3.1 Ga rocks are sporadically exposed
398 within the Eastern Block of the NCC. Wu et al. (2008) conducted in situ analyses and testing
399 of single grain zircon U-Pb in the Anshan complex and concluded that the protoliths of the
400 Tiejiashan and Dongshan gneisses included 3.3–3.1 Ga ancient rocks (Wu et al., 2008).
401 Archean rocks that are ~3.3–~3.1 Ga were also discovered in Caozhuang, Hebei (Liu et al.,
402 1990; Nutman et al., 2011). Therefore, there was indeed a ~3.1 Ga tectonic-magmatic event in
403 the Mesoarchean on the North China Craton. In addition, the 2.6–2.5 Ga rocks are the most
404 widely distributed on the North China Craton with records in both TTGs and metamorphic
405 supracrustal rocks (Zhao et al., 2001b; Yang et al., 2008; Liu et al., 2009; Diwu et al., 2011;
406 Geng et al., 2012; Wan et al., 2012a).
407 Table 2
408 In summary, all these geochronological data from the TTGs, granites, diorite and
409 supracrustal rocks from the basement of the BBB suggest two magmatic events during the
410 Mesoarchean–Neoarchean eras with magmatism occurring at ~3.1 Ga and 2.6–2.5 Ga (Table
411 2).
412
413 **5.2 Crustal accretion and reworking of the BBB basement**
414 The zircon Lu-Hf system is usually used to track the origin of magma and to constrain the
415 time of crust-mantle differentiation (Zeh et al., 2010). Basic rocks are formed by partial melting
416 of the depleted mantle, and intermediate-acid rocks are formed by partial melting of the middle
417 and lower crust originating from the depleted mantle. Basically, if the age of the Hf model, is
418 much higher than the crystallization age of the magma, this indicates a long residence period
419 of the crust after the magma separated from the depleted mantle. On the other hand, if the Hf
420 model age is close to the crystallization age, the parent rock is considered to be a juvenile rock
421 or mantle-derived rock with a short crustal residence time. In this study, the sources of TTG,

granite, and upper crust were acidic, and a two-stage Hf model age is used. The Lu/Hf fractionation index ($f_{Lu/Hf}$) of the lower crust represents the time when the magma was extracted from the depleted mantle (Wu et al., 2016; Wu et al., 2007).

Zircon Lu–Hf data from the Precambrian basement of the Jiyang depression are first reported and discussed in this study to decipher the crustal evolution of the BBB basement, as shown in the ε_{Hf} (t) values versus zircon formation age diagram (Fig.8). Fig.8 shows that magmatic zircons of ~3.1 Ga and 2.6–2.5 Ga ages from the BBB basement have variable Hf isotope compositions. Almost all ~3.1 Ga zircons in samples CHG12-2 and CHG14-2 have positive $\varepsilon_{Hf}(t)$ values from 0.56 to 8.27 and T_{DM1} model ages of 3.33–3.03 Ga, which are slightly older than their crystallization ages of ~3.1 Ga. In addition, most zircons with ~3.1 Ga ages from supracrustal rock (sample CH917-3) have positive $\varepsilon_{Hf}(t)$ values from 1.00 to 12.67 and T_{DM1} model ages of 3.27–2.81 Ga, and two zircons have negative $\varepsilon_{Hf}(t)$ values from sample CH917-3. The single-stage zircon Hf model ages with ~3.1 Ga U-Pb ages are concentrated between 3.3 Ga and 3.1 Ga (Fig. 9a), which is the same as the Hf model age of ~3.1 Ga Archean rocks in Eastern Hebei and Western Liaoning (Fig. 9b). These results suggest that the ~3.1 Ga magmatic rocks were derived from the depleted mantle. Nearly all of the late Neoarchean magmatic zircons from the TTGs and granites with ages of 2.6–2.5 Ga have negative $\varepsilon_{Hf}(t)$ values of -12.87 ~ -0.07, and T_{DM2} model ages of 3.78 ~ 2.96 Ga (concentrated at 3.6 Ga–3.0 Ga) with two peaks at ~3.4 Ga and ~3.1 Ga (Fig.10a), suggesting that the crust was mainly derived from the recycling of older crustal rocks. In addition, in samples CH96-1 and CHX911-1, there are a small number of inherited zircons with core-rim features. The apparent $^{207}Pb/^{206}Pb$ age of zircon cores is ~3.0 Ga, indicating that the Mesoarchean crust (3.0 Ga) was reworked in the late Neoarchean (2.6–2.5 Ga). The late Neoarchean magmatic zircons (2.6–2.5 Ga) from supracrustal rock (CH917-3) also have a T_{DM2} model age with a peak at ~3.38 Ga. The T_{DM2} model ages indicate that the late Neoarchean crust was formed by the reworking of the pre-existing ~3.3 Ga crust, which is different from previous studies on the Archean rocks around of the BBB. The Archean rocks with 2.6–2.5 Ga ages around of the BBB have T_{DM2} model ages concentrated 2.9–2.7 Ga (Fig. 10b). It means that the late Neoarchean crust (2.6–2.5 Ga) around the BBB was mainly derived from 2.8–2.7 Ga crust with some juvenile crustal addition at the end of the Neoarchean (Wan et al., 2010; Diwu et al., 2011; Geng et al., 2012; Wan et al., 2012a;

Wang et al., 2014). A few magmatic zircons in 2.6–2.5 Ga rocks with positive $\varepsilon_{Hf}(t)$ values close to those of the contemporary depleted mantle and T_{DM1} model ages of ~2.9 Ga indicate that minor juvenile additions may have contributed to crustal evolution (Wu et al., 2013).

In summary, the zircon Hf isotope data presented in this study indicate that the basement of the BBB experienced major juvenile crustal growth at ~3.3–3.0 Ga and that the old crust was reworked at 2.6–2.5 Ga. It is worth noting that previous studies found magmatic zircons with negative $\varepsilon_{Hf}(t)$ values in 2.5 Ga rocks, indicating that some of the 2.5 Ga rocks may have been derived from the remelting of the Mesoarchean crust (Zhai, 2014). However, this is the first study in which the magmatic zircons in ~2.5 Ga rocks all have negative Hf isotope values.

5.3 Implications for the Archean crustal evolution of the eastern NCC

The Archean crustal evolution of the Eastern Block has been a controversial issue. Previous studies proposed that the Neoarchean basement rocks of the NCC underwent a large-scale tectono-thermal event at 2.6 – 2.5 Ga (Yang et al., 2008; Wang et al., 2012; Wu et al., 2013), which led some researchers to argue that the major crustal growth of the NCC occurred at ~2.5 Ga (Liu et al., 2009; Diwu et al., 2011). However, an increasing number of 2.8–2.7 Ga rocks have been discovered in the eastern NCC, many of which have 2.8–2.7 Ga model ages based on whole-rock Nd and zircon Hf isotopes (Kröner et al., 2005; Polat et al., 2006; Jahn et al., 2008; Wan et al., 2011; Wu et al., 2013; Yang et al., 2013; Zhu et al., 2013; Wu et al., 2014). These results have led to proposals that both the early Neoarchean (2.8–2.7 Ga) and the late Neoarchean (2.6–2.5 Ga) were important periods of continental crust accretion in the NCC. The 2.8–2.7 Ga tectono-thermal event was of global significance, as it can be found in the Superior, South African, Western Greenland, Baltic and Yilgarn Cratons (Bateman et al., 2001; Crowley, 2002; Poujol et al., 2003; Rino et al., 2004; Bibikova et al., 2005; Percival et al., 2006). The difference is that the 2.8–2.7 Ga accretion event on the NCC was strongly reworked by the 2.6–2.5 Ga event (Wan et al., 2011; Zhai and Santosh, 2011; Wang et al., 2016).

On the NCC, there were still multiple tectonic-magmatic thermal events, such as ~2.9 Ga, ~3.1 Ga, ~3.3 Ga, ~3.6 Ga, and >~3.8 Ga (Song et al., 1996; Zheng et al., 2004; Wu et al., 2008; Wan et al., 2012b; Xie et al., 2014), based on studies of whole-rock Sm-Nd isotopes, zircon Lu-Hf isotopes, detrital zircon U-Pb ages and xenoliths. However, there has hitherto been no

report on the large-scale remelting of the pre-Neoarchean crust during the 2.6–2.5 Ga tectonic-thermal event. Our data show that almost all zircons with ~2.5 Ga age exhibit negative $\varepsilon_{Hf}(t)$ values, and the corresponding T_{DM2} ages are predominantly ~3.4 – 3.0 Ga, which indicates that the Mesoarchean and Paleoarchean crust was also remelted during the ~2.5 Ga tectonic thermal event. Additionally, in this study, we obtained a magma emplacement age of ~3.1 Ga from two TTG gneiss samples (CHG12-2 and CHG14-2) and one metamorphic supracrustal rock sample (CH917-3), indicating that there are Mesoarchean rocks within the basement of the BBB. Moreover, the magmatic zircons in these ~3.1 Ga rocks display positive $\varepsilon_{Hf}(t)$ values and T_{DM1} ages of 3.4–3.0 Ga, indicating that the Paleoarchean crustal accretion events occurred within the basement of the BBB. Previous studies have confirmed that Mesoarchean and Paleoarchean rocks (>3.0 Ga) are occasionally found in Caozhuang, Hebei (Liu et al., 1992) and Anshan, Liaoning (Song et al., 1996; Wan et al., 2005; Wu et al., 2008), Xinyang, Henan (Zheng et al., 2009) and Jiaozuo, Henan (Gao et al., 2006). In the Jiaobei area, the Hf isotope model ages of zircons in some 2.8–2.7 Ga rocks range from ~3.4 Ga to ~3.1 Ga, which represents the remelting of Paleoarchean and Mesoarchean continental crustal materials during the 2.8–2.7 Ga period (Wu et al., 2014).

In summary, in the Eastern Block of the North China Craton, the Mesoarchean and Paleoarchean crust is mainly distributed in the basement and peripheral outcrops of the BBB, and they underwent remelting at ~3.1 Ga, 2.8–2.7 Ga and 2.6–2.5 Ga.

5.4 Tectonic implications

In the NCC 2.6–2.5 Ga rocks including TTGs and metamorphic crustal rocks are widely distributed. However, the tectonic nature of Neoarchean (~2.5 Ga) tectonic thermal events remains controversial. Some have argued that there was a magmatic arc environment at 2.6–2.5 Ga in the eastern part of the NCC because most ~2.5 Ga TTG rocks exhibit calc-alkaline characteristics similar to modern island arcs (Jahn et al., 2008; Peng et al., 2012b; Wang et al., 2012; Liu et al., 2013; Sun et al., 2020). However, the island-arc model cannot explain the lack of andesite in the Archean greenstone belt, ~1600℃ high temperature formation environment of komatiite, large-scale TTG rocks, dome structure style, and anticlockwise P-T path (Zhao, 2014 and references therein). Others have proposed a mantle plume model, which can

reasonably explain large-scale Archean TTG rocks in a short time, dome structural styles, anticlockwise P-T paths, and the lack of blueschists and double metamorphic zones, which are typical characteristics of island-arc subduction zones (Zhao et al., 2001b; Yang et al., 2008; Geng et al., 2012; Wu et al., 2012; Zhao, 2014). Furthermore, rocks derived from a mantle plume are generally distributed over a broad area, whereas island arc rocks tend to be preserved as linear structural belts. Archean greenstone belts in the North China Craton are broadly distributed around the TTG gneiss dome, which is more consistent with a mantle plume origin (Zhao, 2014; Zhao et al., 2021).

Recently, Zhao et al. (2021) proposed a mantle plume-derived oceanic plateau model, which can explain the origin of bimodal volcanic rock assemblages in Archean greenstone belts. In this model, tholeiite and ultrabasic komatiite were derived from partial melting of the head and tail of a mantle plume, respectively. Felsic dacite, rhyolitic dacite and rhyolite are partial melt products of the crust caused by the thermal anomaly of the mantle plume (Zhao and Zhang, 2021). However, the main range of influence of the ~2.5 Ga mantle plume remains unclear.

Our study reveals that ~2.5 Ga TTGs and granites were derived from partial melting of the Mesoarchean and Paleoarchean crust (3.4–3.0 Ga) in the basement of the BBB, which has not been reported before in studies of the NCC. In previous studies, only some zircons with negative $\varepsilon_{Hf}(t)$ values and older Hf model ages were found in ~2.5 Ga rocks in the peripheral outcrops of the BBB. The crystallization ages of rocks around the BBB are mainly concentrated around 2.8-2.7 Ga and 2.6-2.5 Ga (Fig.11). Therefore, we propose that BBB in the Eastern Block of the NCC is an area with considerable mantle plume activity around 2.5 Ga. This mantle plume activity, would have resulted in greater uplift and lithospheric heating in the Bohai Bay Basin region resulting in remelting of both the Neoarchean crust and the Mesoarchean and Paleoarchean crust (3.4–3.0 Ga). However, less remelting would have occurred in the Mesoarchean and Paleoarchean crust than in the Neoarchean crust as the latter would have mainly remelted without mantle plume activity. Moreover, the eastern ancient terrane of the NCC proposed by Wan et al. (2016) is mostly located in the BBB and its periphery (Wan et al., 2016). This may have been the vital area of the eastern crust of the NCC during 2.5 Ga period.

6. Conclusion

Based on new SHRIMP zircon U-Pb, LA-ICP-MS zircon U-Pb and Lu-Hf isotope data obtained from Archean rocks in the basement of the BBB, we present the following major conclusions:

(1) Magmatic zircon U-Pb data suggest that the TTGs, granites and sources of supracrustal rocks of the basement beneath the BBB formed at ~3.1 Ga and 2.6–2.5 Ga.

(2) Zircon Lu-Hf data revealed a major crustal growth event during 3.4–3.0 Ga with the addition of old crustal materials, whereas the ~3.1 Ga and ~2.5 Ga tectono-magmatic events in the BBB mostly involved in crustal reworking.

(3) The Eastern Block of the North China Craton may have been significantly influenced by a mantle plume ~2.5 Ga, and the area with the most intensive the mantle plume activity might have been located beneath the BBB and peripheral areas.

Acknowledgements

We thank Qiqiu Yang for help with the SHRIMP zircon U-Pb analyses, Jinliang Gao for help with Lu-Hf analyses, Shuangrong Zhang for LA-ICP-MS zircon U-Pb analyses in Beijing GeoAnalysis Co., Ltd. (Beijing, China). This study was supported by Shandong Provincial Natural Science Foundation, China (ZR202102250002; ZR2012DL10), National Natural Science Foundation of China Project(41302102; 4177020732) and the Fundamental Research Funds for the Central Universities(15CX05007A).

References

Bai, X., Liu, S.W., Guo, R.R., Wang, W., 2016. A Neoarchean arc–back-arc system in Eastern Hebei, North China Craton: Constraints from zircon U–Pb–Hf isotopes and geochemistry of dioritic–tonalitic–trondhjemitic–granodioritic (DTTG) gneisses and felsic paragneisses. Precambr. Res. 273, 90-111.

Bateman, R., Costa, S., Swe, T., Lambert, D., 2001. Archaean mafic magmatism in the Kalgoorlie area of the Yilgarn Craton, Western Australia: a geochemical and Nd isotopic study of the petrogenetic and tectonic evolution of a greenstone belt. Precambr. Res. 108(1), 75-112.

Bibikova, E.V., Petrova, A., Claesson, S., 2005. The temporal evolution of sanukitoids in the Karelian Craton, Baltic Shield: an ion microprobe U–Th–Pb isotopic study of zircons. Lithos 79(1), 129-145.

Black, L.P., Kamo, S.L., Allen, C.M., Davis, D.W., Aleinikoff, J.N., Valley, J.W., Mundil, R., Campbell, I.H., Korsch, R.J., Williams, I.S., Foudoulis, C., 2004. Improved $^{206}Pb/^{238}U$ microprobe geochronology by the monitoring of a trace-element-related matrix effect; SHRIMP, ID–TIMS,

ELA–ICP–MS and oxygen isotope documentation for a series of zircon standards. Chem. Geol. 205(1), 115-140.

Crowley, J.L., 2002. Testing the model of late Archean terrane accretion in southern West Greenland: a comparison of the timing of geological events across the Qarliit nunaat fault, Buksefjorden region. Precambr. Res. 116(1), 57-79.

Diwu, C.R., Sun, Y., Guo, A.L., Wang, H.L., Liu, X.M., 2011. Crustal growth in the North China Craton at ~2.5Ga: Evidence from in situ zircon U–Pb ages, Hf isotopes and whole-rock geochemistry of the Dengfeng complex. Gondwana Res. 20(1), 149-170.

Du, L.L., Zhuang, Y.X., Yang, C.H., Wan, Y.S., Wand, X.S., 2003. Characters of zircons in the Mengjiatun Formation in Xintai of Shandong and their chronological significance. Acta Geol. Sin. 77, 359-366 (in Chinese with English abstract).

Gao, L.Z., Zhao, T., Wan, Y.S., Zhao, X., Ma, Y.S., Yang, S.Z., 2006. Report on 3.4 Ga SHRIMP Zircon Age from the Yuntaishan Geopark in Jiaozuo, Henan Province. Acta Geol. Sin. 80(1), 52-57.

Geng, Y.S., Du, L.L., Ren, L.D., 2012. Growth and reworking of the early Precambrian continental crust in the North China Craton: Constraints from zircon Hf isotopes. Gondwana Res. 21(2–3), 517-529.

Geng, Y.S., Liu, F.L., Yang, C.H., 2006. Magmatic Event at the End of the Archean in Eastern Hebei Province and Its Geological Implication. Acta Geol. Sin. 80(6), 819-833.

Grant, M.L., Wilde, S.A., Wu, F.Y., Yang, J.H., 2009. The application of zircon cathodoluminescence imaging, Th-U-Pb chemistry and U-Pb ages in interpreting discrete magmatic and high-grade metamorphic events in the North China Craton at the Archean/Proterozoic boundary. Chem. Geol. 261, 155-171.

Griffin, W.L., Pearson, N.J., Belousova, E., Jackson, S.E., van Achterbergh, E., O'Reilly, S.Y., Shee, S.R., 2000. The Hf isotope composition of cratonic mantle: LAM-MC-ICPMS analysis of zircon megacrysts in kimberlites. Geochim. Cosmochim. Acta 64(1), 133-147.

Guo, R.R., Liu, S.W., Santosh, M., Li, Q.G., Bai, X., Wang, W., 2013. Geochemistry, zircon U–Pb geochronology and Lu–Hf isotopes of metavolcanics from eastern Hebei reveal Neoarchean subduction tectonics in the North China Craton. Gondwana Res. 24(2), 664-686.

Guo, R.R., Liu, S.W., Wyman, D., Bai, X., Wang, W., Yan, M., Li, Q.G., 2015. Neoarchean subduction: A case study of arc volcanic rocks in Qinglong-Zhuzhangzi area of the Eastern Hebei Province, North China Craton. Precambr. Res. 264, 36-62.

Guo, Z., Wilson, M., Liu, J., Mao, Q., 2006. Post-collisional, potassic and ultrapotassic magmatism of the northern Tibetan Plateau: Constraints on characteristics of the mantle source, geodynamic setting and uplift mechanisms. J. Petrol. 47(6), 1177-1220.

Jahn, B.M., Liu, D.Y., Wan, Y.S., Song, B., Wu, J.S., 2008. Archean crustal evolutionof the Jiaodong Peninsula, China, as revealed by zircon SHRIMP geochronology, elemental and Nd-isotope geochemistry. Am. J. Sci. 308, 232-269.

Kröner, A., Cui, W.Y., Wang, W.Y., Wang, C.Q., Nemchin, A.A., 1998. Single zircon ages from high-grade rocks of the Jianping Complex, Liaoning Province, NE China. J. Asian Earth Sci. 16, 519-532.

Kröner, A., Wilde, S., O'Brien, P.J., Li, J.H., Passchier, C.W., Walte, N.P., Liu, D.Y., 2005. Field relationships, geochemistry, zircon ages and evolution of a late Archaeanto Palaeoproterozoic lower crustal section in the Hengshan Terrain of NorthernChina. Acta Geol. Sin. 79, 605-629.

Li, J.J., Shen, B.F., 2000. Geochronology of Precambrian continent crust in Liaoning Province and

Jilin Province. Prog. Precambr. Res. 23, 249-255 (in Chinese with English abstract).
Li, T.S., Zhai, M.G., Peng, P., Chen, L., Guo, J.H., 2010. Ca. 2.5 billions year old coeval ultramafic–mafic and syenitic dykes in Eastern Hebei: Implications for cratonization of the North China Craton. Precambr. Res. 180(3), 143-155.
Li, X.H., Qi, C.S., Liu, Y., Liang, X.R., Tu, X.L., Xie, L.W., Yang, Y.H., 2005. Petrogenesis of the Neoproterozoic bimodal volcanic rocks along the western margin of the Yangtze Block: new constraints from Hf isotopes and Fe/Mn ratios. Chin. Sci. Bull. 50, 2481-2486.
Li, Z.X., Zuo, Y.H., Qiu, N.S., Gao, J.,2017. Meso–Cenozoic lithospheric thermal structure in the Bohai Bay Basin, eastern North China Craton. Geosci. Front. 8(5), 977-987.
Liou, P., Guo, J.H., Huang, G.Y., Fan, W.B., 2019. 2.9 Ga magmatism in Eastern Hebei, North China Craton. Precambr. Res. 326, 6-23.
Liu, D.Y., Nutman, A.P., Compston, W., Wu, J.S., Shen, Q.H., 1992. Remnants of 3800 Ma crust in the Chinese part of the Sino-Korean Craton. Geology 20, 339-342.
Liu, D.Y., Shen, Q.H., Zhang, Z.Q., Jahn, B.M., Auvray, B., 1990. Archean crustal evolution in China: U-Pb geochronology of the Qianxi Complex. Precambr. Res. 48(3), 223-244.
Liu, D.Y., Wilde, S.A., Wan, Y.S., Wang, S.Y., Valley, J.W., Kita, N., Dong, C.Y., Xie, H.Q., Yang, C.X., Zhang, Y.X., Gao, L.Z., 2009. Combined U–Pb, hafnium and oxygen isotope analysis of zircons from meta-igneous rocks in the southern North China Craton reveal multiple events in the Late Mesoarchean–Early Neoarchean. Chem. Geol. 261(1), 140-154.
Liu, D.Y., Wilde, S.A., Wan, Y.S., Wu, J.S., Zhou, H.Y., Dong, C.Y., Yin, X.Y., 2008. New U-Pb and Hf isotopic data confirm Anshan as the oldest preserved segment of the North China Craton. Am. J. Sci. 308, 200-231.
Liu, J., Zhang, J., Yin, C.Q., Cheng, C.Q., Liu, X.G., Zhao, C., Chen, Y., Wang, X., 2020. Synchronous A-type and adakitic granitic magmatism at ca. 2.2 Ga in the Jiao–Liao–Ji belt, North China Craton: Implications for rifting triggered by lithospheric delamination. Precambr. Res. 342(15), 105629.
Liu, J.H., Liu, F.L., Ding, Z.J., Liu, C.H., Yang, H., Liu, P.H., Wang, F., Meng, E., 2013. The growth, reworking and metamorphism of early Precambrian crust in the Jiaobei terrane, the North China Craton: Constraints from U–Th–Pb and Lu–Hf isotopic systematics, and REE concentrations of zircon from Archean granitoid gneisses. Precambr. Res. 224, 287-303.
Liu, S.W., Santosh, M., Wang, W., Bai, X., Yang, P.T., 2011. Zircon U-Pb chronology of the Jianping Complex: implications for the Precambrian crustal evolution history of the northern margin of North China Craton. Gondwana Res. 20, 48-63.
Liu, Y.S., Gao, S., Hu, Z.C., Gao, C.G., Zong, K.Q., Wang, D.B., 2010. Continental and Oceanic Crust Recycling-induced Melt–Peridotite Interactions in the Trans-North China Orogen: U–Pb Dating, Hf Isotopes and Trace Elements in Zircons from Mantle Xenoliths. J. Petrol. 51(1-2), 537-571.
Lu, S.N., Zhao, G.C., Wang, H.C., Hao, G.J., 2008. Precambrian metamorphic basement and sedimentary cover of the North China Craton: A review. Precambr. Res. 160, 77-93.
Lu, X.P., Wu, F.Y., Lin, J.Q., Sun, D.Y., Zhang, Y.B., Guo, C.L., 2004. Geochronological successions of the early Precambrian granitic magmatism in southern Liaodong peninsula and its constraints on tectonic evolution of the north China craton. Chin. J. Geol. 39(1), 123-138.
Lv, B., Zhai, M.G., Li, T.S., Peng, P., 2012. Zircon U–Pb ages and geochemistry of the Qinglong volcano-sedimentary rock series in Eastern Hebei: Implication for ~2500Ma intra-continental rifting in the North China Craton. Precambr. Res. 208-211, 145-160.
Meng, E., Liu, F.L., Liu, J.H., Liu, P.H., Cui, Y., Liu, C.H., Yang, H., Wang, F., Shi, J.R., Kong, Q.B., Lian,

T., 2013. Zircon U–Pb and Lu–Hf isotopic constraints on Archean crustal evolution in the Liaonan Complex of northeast China. Lithos 177, 164-183.

Meng, F.C., Cui, Y., Cao, Y.C., Qiu, L.W., Wei, J.Y., Qu, Z.J., Liu, J.Q., 2017. A discovery of ~3.1Ga basement in the Bohai Bay Basin. Acta Geol. Sin. 91(4), 1495-1496.

Nutman, A.P., Wan, Y., Du, L., Friend, C.R.L., Dong, C., Xie, H., Wang, W., Sun, H., Liu, D., 2011. Multistage late Neoarchaean crustal evolution of the North China Craton, eastern Hebei. Precambr. Res. 189(1–2), 43-65.

O'Connor, J.T., 1965. A classification for quartz-rich igneous rocks based on feldspar ratios. U.S. Geol. Surv. Prof. Pap. 525, 79-84.

Peng, P., Guo, J., Zhai, M., Windley, B.F., Li, T., Liu, F., 2012a. Genesis of the Hengling magmatic belt in the North China Craton: Implications for Paleoproterozoic tectonics. Lithos 148(0), 27-44.

Peng, T.P., Fan, W.M., Peng, B.X., 2012b. Geochronology and geochemistry of late Archean adakitic plutons from the Taishan granite–greenstone Terrain: Implications for tectonic evolution of the eastern North China Craton. Precambr. Res. 208-211, 53-71.

Percival, J.A., Sanborn-Barrie, M., Skulski, T., Stott, G.M., Helmstaede, H., White, D.J., 2006. Tectonic evolution of the western Superior Province from NATMAP and Lithoprobe studies. Can. J. Earth Sci. 43, 1085-1117.

Polat, A., Li, J.H., Fryer, B., Kusky, T., Kerrich, R., Gagnon, J., Zhang, S., 2006. Geochemical characteristics of the Neoarchean(2800~2700Ma) Taishan greenstone belt, North China Craton: Evidence for plume-craton interaction. Chem. Geol. 230, 60-87.

Poujol, M., Robb, L.J., Anhaeusser, C.R., Gericke, B., 2003. A review of the geochronological constraints on the evolution of the Kaapvaal Craton, South Africa. Precambr. Res. 127(1), 181-213.

Rino, S., Komiya, T., Windley, B.F., Katayama, I., Motoki, A., Hirata, T., 2004. Major episodic increases of continental crustal growth determined from zircon ages of river sands; implications for mantle overturns in the Early Precambrian. Phys Earth Planet In. 146(1), 369-394.

Shen, Q.H., Zhao, Z.R., Song, B., Song, H.X., 2007. Geology, petrochemistry and SHRIMP zircon U-Pb dating of the Mashan and Xueshan granitoids in Yishui County, Shandong province. Geol. Rev. 53(2), 180-186 (in Chinese with English abstract).

Sláma, J., Košler, J., Condon, D.J., Crowley, J.L., Gerdes, A., Hanchar, J.M., Horstwood, M.S.A., Morris, G.A., Nasdala, L., Norberg, N., Schaltegger, U., Schoene, B., Tubrett, M.N., Whitehouse, M.J., 2008. Plešovice zircon – A new natural reference material for U–Pb and Hf isotopic microanalysis. Chem. Geol. 249(1), 1-35.

Söderlund, U., Patchett, P.J., Vervoort, J.D., Isachsen, C.E., 2004. The ^{176}Lu decay constant determined by Lu–Hf and U–Pb isotope systematics of Precambrian mafic intrusions. Earth Planet. Sci. Lett. 219(3), 311-324.

Song, B., Nutman, A.P., Liu, D.Y., Wu, J.S., 1996. 3800 to 2500 Ma crustal evolution in the Anshan area of Liaoning Province, northeastern China. Precambr. Res. 78(1–3), 79-94.

Song, B.R., Hu, Y.J., Bian, S.Z., Han, H.D., Cui, X.D., and Zhang, J., 2011. Researvoir characeristics of the crystal basement in the Xinglongtai buried-hill, Liaohe Depression. Acta Petrol. Sin. 32(1), 77-82 (in Chinese with English abstract).

Sun, G.Z., Liu, S.W., Gao, L., Hu, Y.L., Guo, R.R., 2020. Origin of late Neoarchean granitoid diversity in the Western Shandong province, North China Craton. Precambr. Res. 339, 105620.

Tang, J., Zheng, Y.F., Wu, Y.B., Bing, G., Liu, X., 2007. Geochronology and geochemistry of

metamorphic rocks in the jiaobei terrane: constraints on its tectonic affinity in the sulu orogen. Precambr. Res. 152(1-2), 48-82.

Wan, Y.S., Dong, C.Y., Liu, D.Y., Kröner, A., Yang, C.H., Wang, W., Du, L., Xie, H.Q., Ma, M.Z., 2012a. Zircon ages and geochemistry of late Neoarchean syenogranites in the North China Craton: A review. Precambr. Res. 222–223, 265-289.

Wan, Y.S., Liu, D.Y., Nutman, A., Zhou, H., Dong, C.A., Yin, X.Y., Ma, M.Z., 2012b. Multiple 3.8–3.1 Ga tectono-magmatic events in a newly discovered area of ancient rocks (the Shengousi Complex), Anshan, North China Craton. J. Asian Earth Sci. 54-55, 18-30.

Wan, Y.S., Liu, D.Y., Song, B., Wu, J.S., Yang, C.H., Zhang, Z.Q., Geng, Y.S., 2005. Geochemical and Nd isotopic compositions of 3.8 Ga meta-quartz dioritic and trondhjemitic rocks from the Anshan area and their geological significance. J. Asian Earth Sci. 24(5), 563-575.

Wan, Y.S., Liu, D.Y., Wang, S.J., Dong, C.Y., Yang, E.X., Wang, W., Zhou, H.Y., Ning, Z.G., Du, L., Yin, X.Y., Xie, H.Q., Ma, M.Z., 2010. Juvenile magmatism and crustal recycling at the end of the Neoarchean in Western Shandong Province, North China Craton: Evidence from SHRIMP zircon dating. Am. J. Sci. 310(10), 1503-1552.

Wan, Y.S., Liu, D.Y., Wang, S.J., Yang, E.X., Wang, W., Dong, C.Y., Zhou, H.Y., Du, L., Yang, Y.H., Diwu, C.R., 2011. ~2.7Ga juvenile crust formation in the North China Craton (Taishan-Xintai area, western Shandong Province): Further evidence of an understated event from U–Pb dating and Hf isotopic composition of zircon. Precambr. Res. 186, 169-180.

Wan, Y.S, Liu, S.J., Alfred, K., Dong, C.Y., Xie, H.Q., Xie, S.W., Bai, W.Q., Ren, P., Ma, M.Z., Liu, D.Y., 2016. Eastern Ancient Terrane of the North China Craton. Acta Geol. Sin. 90(4), 1082-1096.

Wan, Y.S, Xie, S.W., Yang, C.H., Kröner, A., Ma, M.Z., Dong, C.Y., Du, L.L., Xie, H.Q., Liu, D.Y., 2014a. Early Neoarchean (~2.7 Ga) tectono-thermal events in the North China Craton: A synthesis. Precambr. Res. 247, 45-63.

Wan, Y.S., Zhang, Y.H., Williams, I.S., Liu, D.Y., Dong, C.Y., Fan, R.L., Shi, Y.R., Ma, M.Z., 2013. Extreme zircon o isotopic compositions from 3.8 to 2.5 Ga magmatic rocks from the Anshan area, North China Craton. Chem. Geol. 352, 108-124.

Wan, Y.S, Zhao, X.Z., Wang, Z.J., Liu, D.Y., Kröner, A., Dong, C.Y., Xie, H.Q., Geng, Y.S., Zhang, Y.H., Fan, R.L., Sun, H.Y., 2014b. SHRIMP zircon dating and LA-ICPMS Hf analysis of early Precambrian rocks from drill holes into the basement beneath the Central Hebei Basin, North China Craton. Geosci. Front. 5(4), 471-484.

Wang, D.Y., Wang, Q.B., Liu, X.J., Zhao, M., Hao Y.W., 2019. Characteristics and developing patterns of gneiss buried hill weathering crust reservoir in the sea area of the Bohai Bay basin. Acta Petrol. Sin. 35 (4),1181-1193 (in Chinese with English abstract).

Wang, F., Li, X.P., Chu, H., Zhao, G., 2011a. Petrology and metamorphism of khondalites from the Jining complex, North China craton. Int. Geol. Rev. 53(2), 212-229.

Wang, F., Liu, F.L., Schertl, H.P., Xu, W., Liu, P.H., Tian, Z.H., 2020. Detrital zircon U-Pb geochronology and Hf isotopes of the Liaohe Group, Jiao-Liao-Ji Belt: Implications for the Paleoproterozoic tectonic evolution. Precambr. Res. 340, 105633.

Wang, S.J., Wan, Y.S., Zhang, C.J., Yang, E.X., Song, Z.Y., Wang, L.F., Zhang, F.Z., 2008. New progress made in early Precambrian geology of the Luxi area. Land and Resources of Shandong Province 24(1), 10-20 (in Chinese with English abstract).

Wang, W., Liu, S.W., Bai, X., Yang, P.T., Li, Q.G., Zhang, L.F., 2011b. Geochemistry and zircon U–Pb–Hf isotopic systematics of the Neoarchean Yixian–Fuxin greenstone belt, northern margin of the

North China Craton: Implications for petrogenesis and tectonic setting. Gondwana Res. 20(1), 64-81.

Wang, W., Liu, S.W., Santosh, M., Bai, X., Li, Q.G., Yang, P.T., Guo, R.R., 2013. Zircon U–Pb–Hf isotopes and whole-rock geochemistry of granitoid gneisses in the Jianping gneissic terrane, Western Liaoning Province: Constraints on the Neoarchean crustal evolution of the North China Craton. Precambr. Res. 224, 184-221.

Wang, W., Liu, S.W., Santosh, M., Wang, G.H., Bai, X., Guo, R.R., 2015. Neoarchean intra-oceanic arc system in the Western Liaoning Province: Implications for Early Precambrian crustal evolution in the Eastern Block of the North China Craton. Earth Sci. Rev. 150, 329-364.

Wang, W., Liu, S.W., Wilde, S.A., Li, Q.G., Zhang, J., Bai, X., Yang, P.T., Guo, R.R., 2012. Petrogenesis and geochronology of Precambrian granitoid gneisses in Western Liaoning Province: Constraints on Neoarchean to early Paleoproterozoic crustal evolution of the North China Craton. Precambr. Res. 222-223, 290-311.

Wang, W., Zhai, M.G., Li, T.S., Santosh, M., Zhao, L., Wang, H.Z., 2014. Archean–Paleoproterozoic crustal evolution in the eastern North China Craton: Zircon U–Th–Pb and Lu–Hf evidence from the Jiaobei terrane. Precambr. Res. 241, 146-160.

Wang, W., Zhai, M.G., Wang, S.J., Santosh, M., 2016. Neoarchean crustal evolution in western Shandong Province of the North China Craton: The role of 2.7–2.6 Ga magmatism. Precambr. Res. 285, 170-185.

Wu, F.Y., Yang, Y.H., Xie, L.W., Yang, J.H., Xu, P., 2006. Hf isotopic compositions of the standard zircons and baddeleyites used in U–Pb geochronology. Chem. Geol. 234(1–2), 105-126.

Wu, F.Y., Zhang, Y.B., Yang, J.H., Xie, L.W., Yang, Y.H., 2008. Zircon U–Pb and Hf isotopic constraints on the Early Archean crustal evolution in Anshan of the North China Craton. Precambr. Res. 167, 339-362.

Wu, M.L., Lin, S.F., Wan, Y.S., Gao, J.F., 2016. Crustal evolution of the Eastern Block in the North China Craton: Constraints from zircon U–Pb geochronology and Lu–Hf isotopes of the Northern Liaoning Complex. Precambr. Res. 275, 35-47.

Wu, M.L., Zhao, G.C., Sun, M., Li, S.Z., Bao, Z.A., Tam, P.Y., Eizenhöefer, P.R., He, Y.H., 2014. Zircon U–Pb geochronology and Hf isotopes of major lithologies from the Jiaodong Terrane: Implications for the crustal evolution of the Eastern Block of the North China Craton. Lithos 190-191, 71-84.

Wu, M.L., Zhao, G.C., Sun, M., Li, S.Z., He, Y.H., Bao, Z.A., 2013. Zircon U-Pb geochronology and Hf isotopes of major lithologies from the Yishui Terrane: Implications for the crustal evolution of the Eastern Block, North China Craton. Lithos 170–171, 164-178.

Wu, M.L., Zhao, G.C., Sun, M., Yin, C.Q., Li, S.Z., Tam, P.Y., 2012. Petrology and P–T path of the Yishui mafic granulites: Implications for tectonothermal evolution of the Western Shandong Complex in the Eastern Block of the North China Craton. Precambr. Res. 222-223, 312-324.

Wu, Y.B., Zheng, Y.F., Zhang, S.B., Zhao, Z.F., Wu, F.Y., Liu, X.M., 2007. Zircon U–Pb ages and Hf isotope compositions of migmatite from the North Dabie terrane in China: constraints on partial melting. J. Metamorph. Geol. 25(9), 991-1009.

Xie, S.W., Xie, H.Q., Wang, S.J., Kröner, A., Liu, S.J., Zhou, H.Y., Ma, M.Z., Dong, C.Y., Liu, D.Y., Wan, Y.S., 2014. Ca. 2.9 Ga granitoid magmatism in eastern Shandong, North China Craton: Zircon dating, Hf-in-zircon isotopic analysis and whole-rock geochemistry. Precambr. Res. 255, Part 2, 538-562.

Yang, C.H., Du, L.L., Ren, L.D., Song, H.X., Wan, Y.S., Xie, H.Q., Geng, Y.S., 2013. Delineation of the Ca. 2.7 Ga TTG gneisses in the Zanhuang Complex, North China Craton and its geological implications. J. Asian Earth Sci. 72, 178-189.

Yang, J.H., Wu, F.Y., Wilde, S.A., Zhao, G.C., 2008. Petrogenesis and geodynamics of late Archean magmatism in eastern Hebei eastern North China Craton: Geochronological, geochemical and Nd-Hf isotopic evidence. Precambr. Res. 167(1-2), 125-149.

Yin, C.Q., Zhao, G.C., Wei, C.J., Sun, M., Guo, J.H., Zhou, X.W., 2014. Metamorphism and partial melting of high-pressure pelitic granulites from the Qianlishan Complex: Constraints on the tectonic evolution of the Khondalite Belt in the North China Craton. Precambr. Res. 242, 172-186.

Zeh, A., Gerdes, A., Will, T.M., Frimmel, H.E., 2010. Hafnium isotope homogenization during metamorphic zircon growth in amphibolite-facies rocks: Examples from the Shackleton Range (Antarctica). Geochim. Cosmochim. Acta 74(16), 4740-4758.

Zhai, M.G., 2014. Multi-stage crustal growth and cratonization of the North China Craton. Geosci. Front. 5(4), 457-469.

Zhai, M.G., Bian, A.G., 2000. Amalgamation of the supercontinental of the North China Craton and its break up during late middle Proterozoic. Sci. China, Ser. D. 43, 219-232.

Zhai, M.G., Santosh, M., 2011. The early Precambrian odyssey of the North China Craton: A synoptic overview. Gondwana Res. 20(1), 6-25.

Zhao, G.C., 2014. Precambrian Evolution of the North China Craton. Elsevier, Boston, 95-147.

Zhao, G.C., Cawood, P.A., Wilde, S.A., Lu, L.Z., 2001b. High-Pressure Granulites (Retrograded Eclogites) from the Hengshan Complex, North China Craton: Petrology and Tectonic Implications. J. Petrol. 42(6), 1141-1170.

Zhao, G.C., Sun, M., Wilde, S.A., Li, S.Z., 2005. Late Archean to Paleoproterozoic evolution of the North China Craton: key issues revisited. Precambr. Res. 136(2), 177-202.

Zhao, G.C., Wilde, S.A., Cawood, P.A., Sun, M., 2001a. Archean blocks and their boundaries in the North China Craton: lithological, geochemical, structural and P–T path constraints and tectonic evolution. Precambr. Res. 107(1-2), 45-73.

Zhao, G.C., Zhang G.W., 2021. Origin of continents. Acta Geol. Sin. 95(1), 1-19 (in Chinese with English abstract).

Zhao, Z.R., Song, H.X., Shen, Q.H., Song, B., 2008. Geological and geochemical characteristics and shrimp u-pb zircon dating of the Yinglingshan granite and its xenoliths in Yishui county, Shandong, China. Geol. Bull. China 27(9), 1551-1558 (in Chinese with English abstract).

Zheng, J.P., Griffin, W.L., O'Reilly, S.Y., Lu, F.X., Wang, C.Y., Zhang, M., Wang, F.Z., Li, H.M., 2004. 3.6 Ga lower crust in central China: New evidence on the assembly of the North China craton. Geology 32(3), 229-232.

Zheng, J.P., Griffin, W.L., O'Reilly, S.Y., Zhao, J.H., Wu, Y.B., Liu, G.L., Pearson, N., Zhang, M., Ma, C.Q., Zhang, Z.H., Yu, C.M., Su, Y.P., Tang, H.Y., 2009. Neoarchean (2.7–2.8 Ga) accretion beneath the North China Craton: U–Pb age, trace elements and Hf isotopes of zircons in diamondiferous kimberlites. Lithos 112(3-4), 188-202.

Zhu, X.Y., Zhai, M.G., Chen, F.K., Lyu, B., Wang, W., Peng, P., Hu, B., 2013. ~2.7-Ga Crustal Growth in the North China Craton: Evidence from Zircon U-Pb Ages and Hf Isotopes of the Sushui Complex in the Zhongtiao Terrane. J. Geol. 121(3), 239-254.

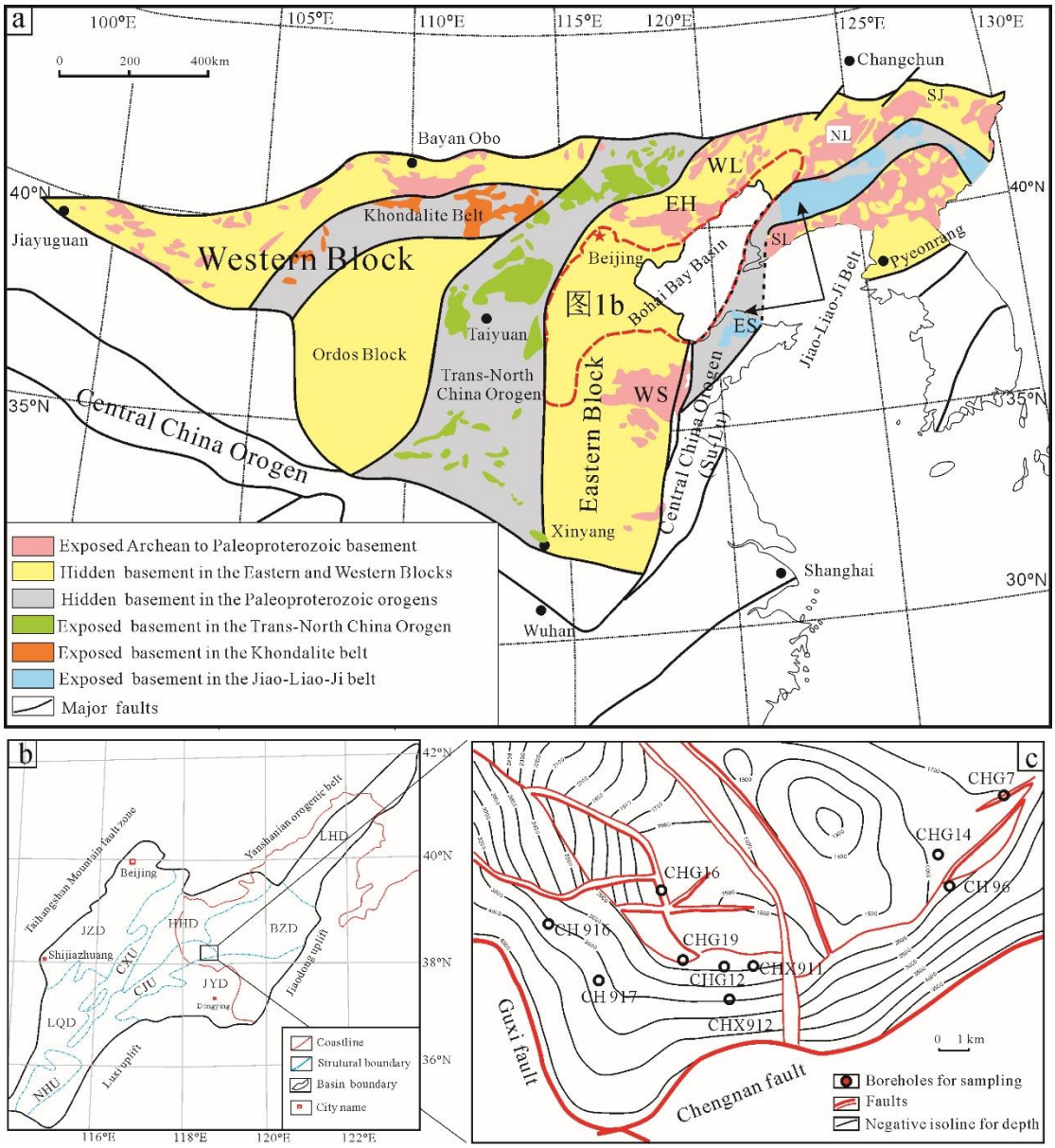

Fig.1 (a) Geological sketch map of the North China(NCC) (Modified after Zhao et al.,2005); (b) Structural units in the Bohai Bay Basin (Modified after Li et al., 2017); (c) Location of boreholes for sampling in the northeastern ChengNing uplift

Abbreviations: EH-Eastern Hebei; NL-Northern Liaoning; SL-Southern Liaoning; WL-Western Liaoning; WS-Western Shandong; ES-Estern Shandong; NL-Norhtern Liaoning; LQS-LinQing depression; JYS-JiYang depression; JZS-JiZhong depression; HHS-HuangHua depression; LHS-LiaoHe depression; XNU-XingNing uplift; CXU-CangXian uplift; CNU-ChengNing uplift

849

850

851 **Fig.2 Drill core photographs of the basement rocks in Jiyang depression of the BBB.** (a, b)
852 Massive Granodiorite. （c）Tonalitic gneiss. (d) Tonalitic gneiss with migmatized felsic veins. (e)
853 Trondhjemitic gneiss. (f) Trondhjemitic gneiss with migmatized felsic spots. (g) Monzogranite. (h)
854 Syenogranite. (i) Leptite

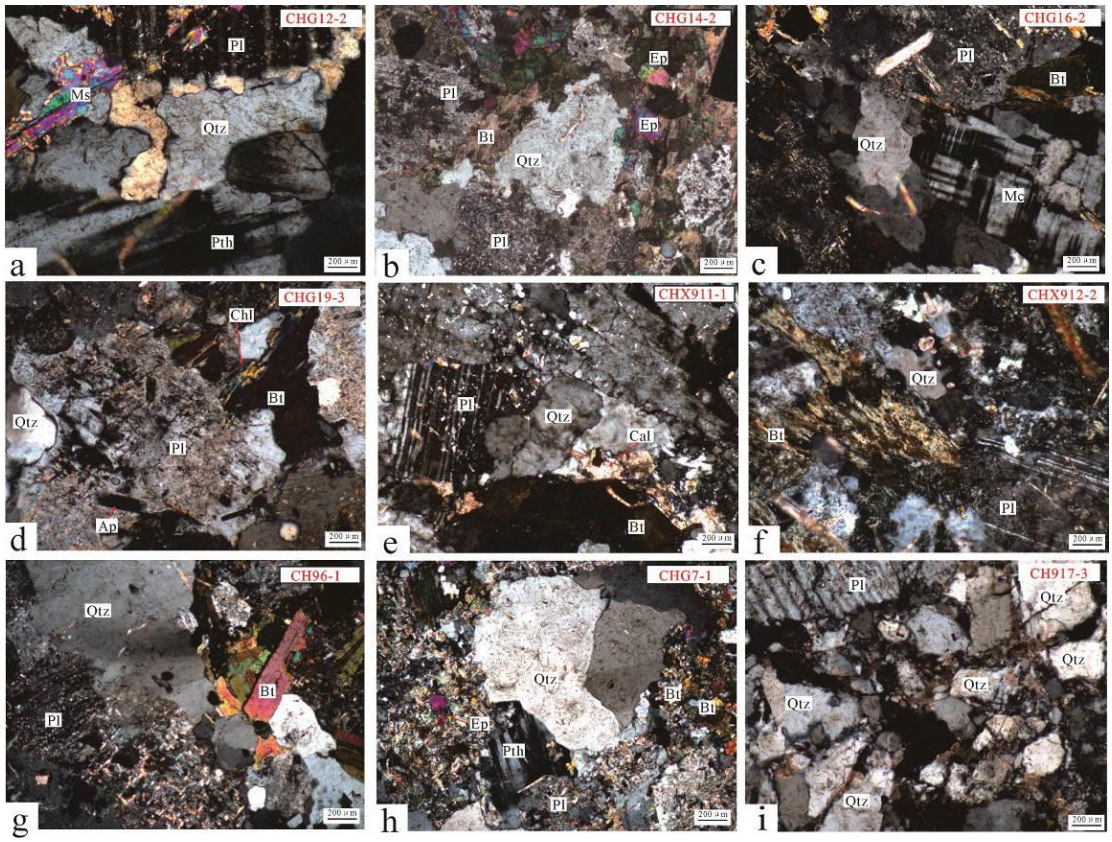

855

Fig.3 Photomicrographs (orthogonal polarized) of the basement rocks in Jiyang depression of the BBB. Hb=hornblende; Bt=biotite; Qtz=quartz; Pl=plagioclase; Pth=perthite; Mc=microline; Kfs=K-feldspar; Zr=zircon; Sp=titanite; Ap=apatite; Ep=epidote; Mag=magnetite; Ser=Sericite; Chl=Chlorite; Ms=muscovite; Cal=Calcite; a.m.=accessory mineral

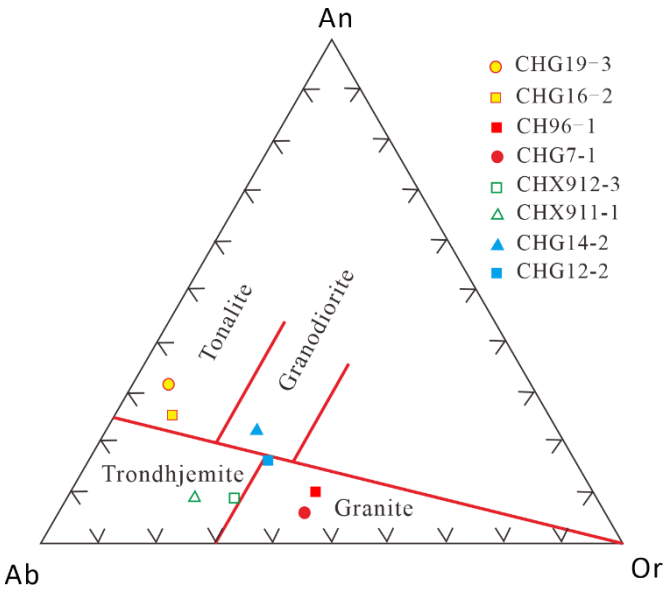

Fig.4 An-Ab-Or diagram of basement rocks from the Jiyang depression of the BBB (Modified after O'Connor, 1965)

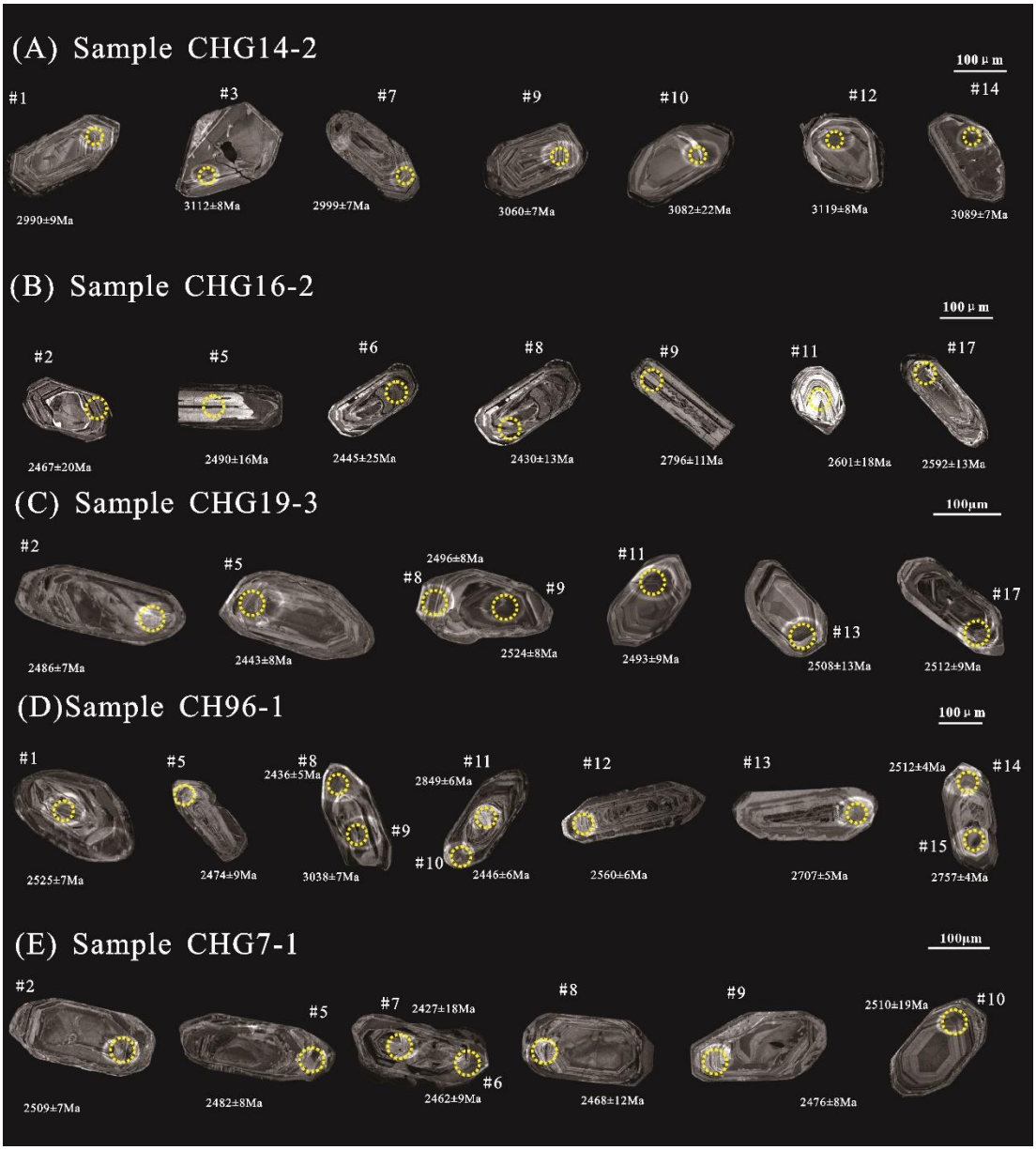

Fig.5 Representative cathodoluminescence (CL) images for zircons from Archean rocks the in Jiyang depression of the BBB.

U-Pb and Lu-Hf analytical spots with the same position, $^{207}Pb/^{206}Pb$ ages, and $\varepsilon_{Hf}(t)$ values are marked

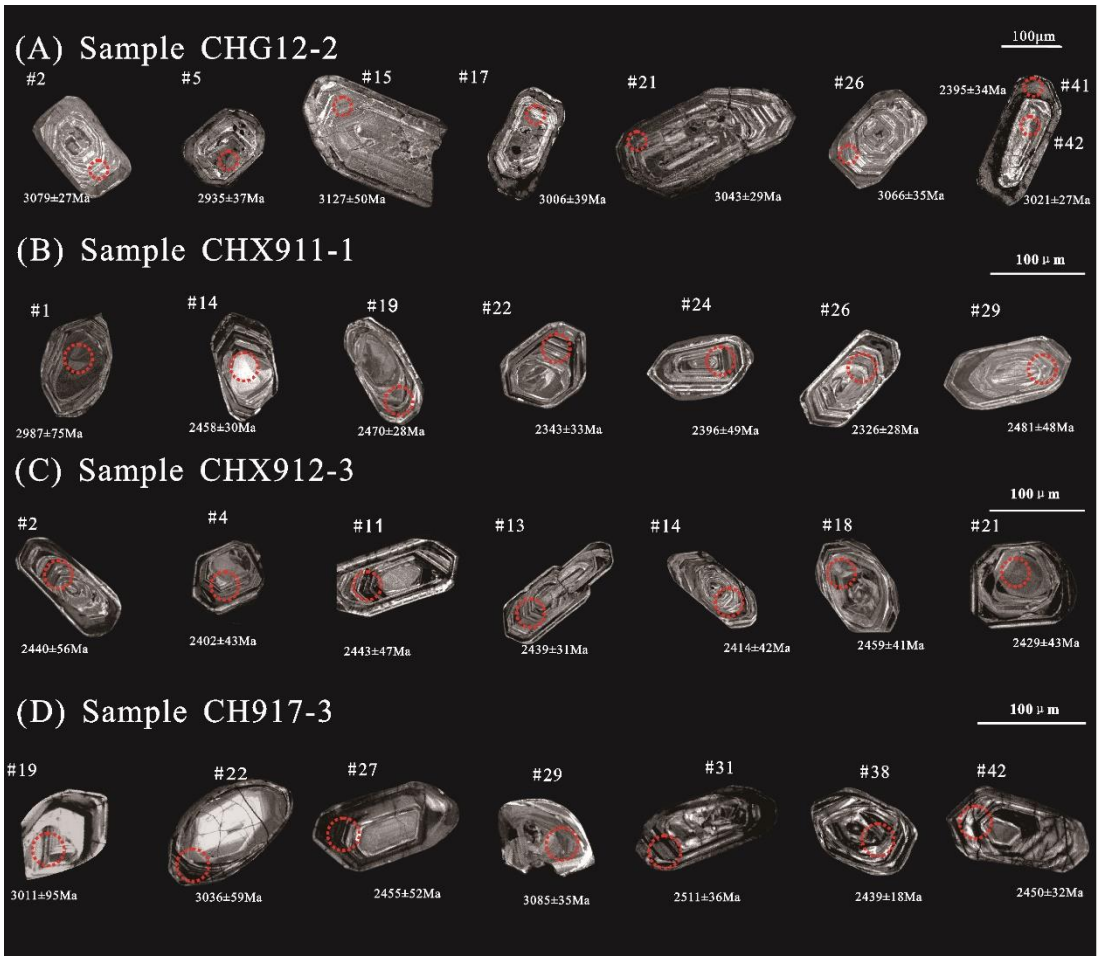

Fig.6 Representative cathodoluminescence(CL) images for zircons from Archean rocks in Jiyang depression of the BBB.

U-Pb and Lu-Hf analytical spots with the same position, $^{207}Pb/^{206}Pb$ ages, and $\varepsilon_{Hf}(t)$ values are marked (continued from Fig. 4)

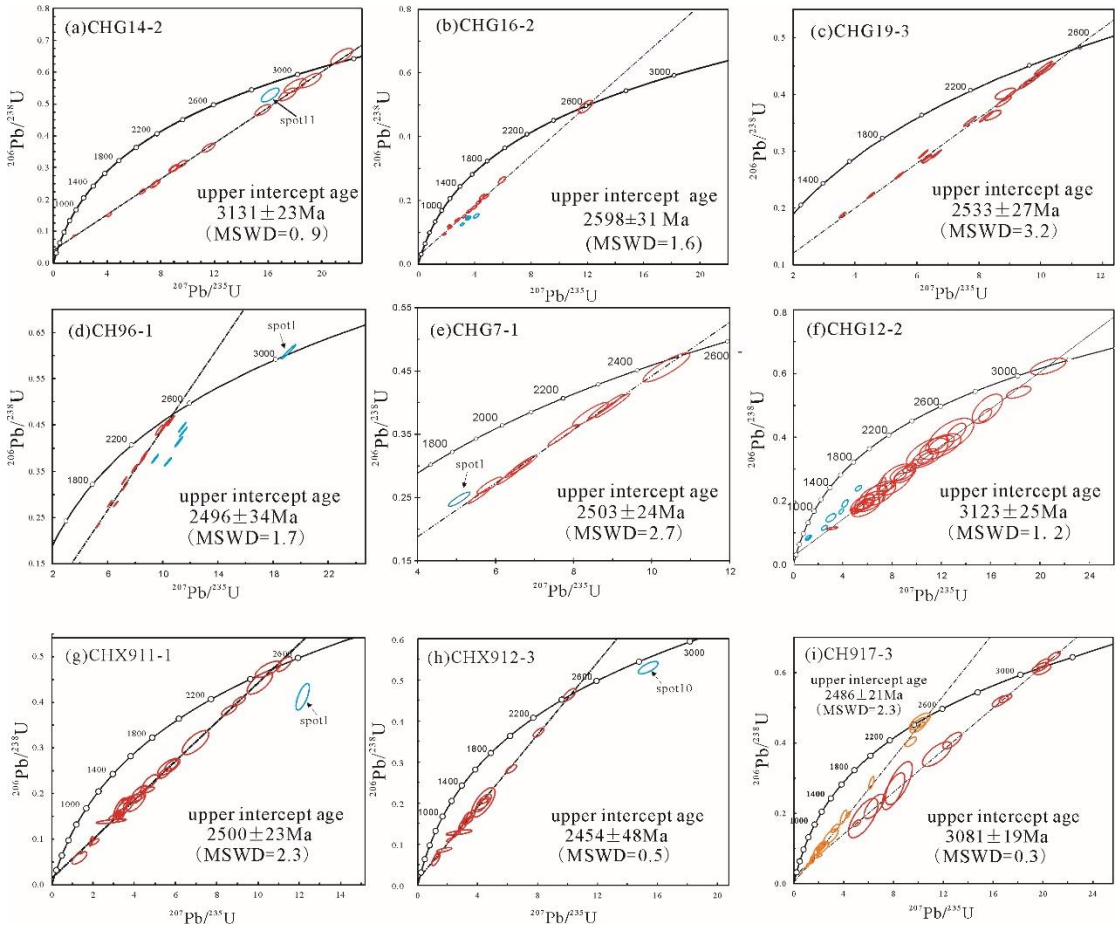

Fig.7 Zircon U-Pb concordia diagrams for basement rocks from the Jiyang depression of the BBB. Data point error ellipses are 2σ. The analytical data are listed in Supplementary Table S1 and S2

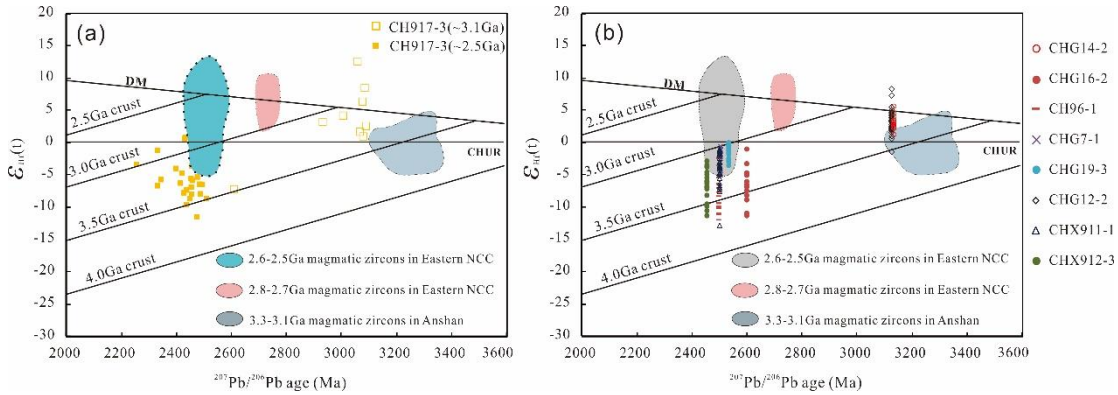

Fig.8 Plots of the zircon ε_{Hf} (t) values versus crystallization (Ma) for the dated samples. (a) Supracrustal rock (Sample CH917-3); (b) TTGs and granites

Data source for zircon ε_{Hf} (t) values and $^{207}Pb/^{206}Pb$ age of 3.3 -3.1 Ga, 2.8 -2.7 Ga and 2.6-2.5 Ga: Wu et al., 2008; Yang et al., 2008; Li et al., 2010; Wan et al., 2011; Wang et al., 2011b; Lv et al., 2012; Peng et al., 2012a; Wang et al., 2012; Liu et al., 2013; Meng et al., 2013; Wang et al., 2013; Wu et al., 2013; Wan et al., 2014b; Guo et al., 2015; Wu et al., 2016; Sun et al., 2020

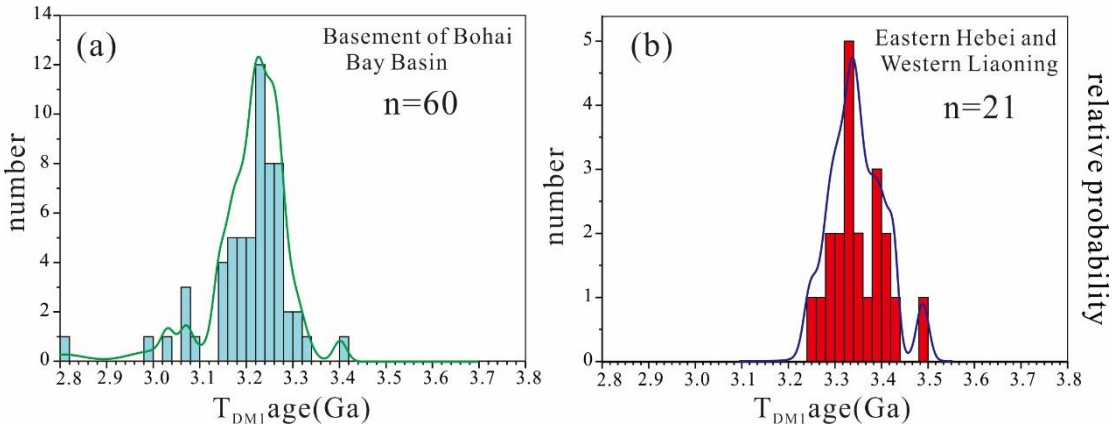

887

888 **Fig.9 Histogram of single-stage Hf model ages with the U-Pb age of ~3.1Ga model ages of magmatic**
889 **zircons from the. (a) Archean basement of the Jiyang depression of BBB; (b) Archean basement of**
890 **the Eastern Hebei and Western Liaoning**

891 Data source for Eastern Hebei and Western Liaoning: Wu et al., 2008; Liou et al., 2019

892

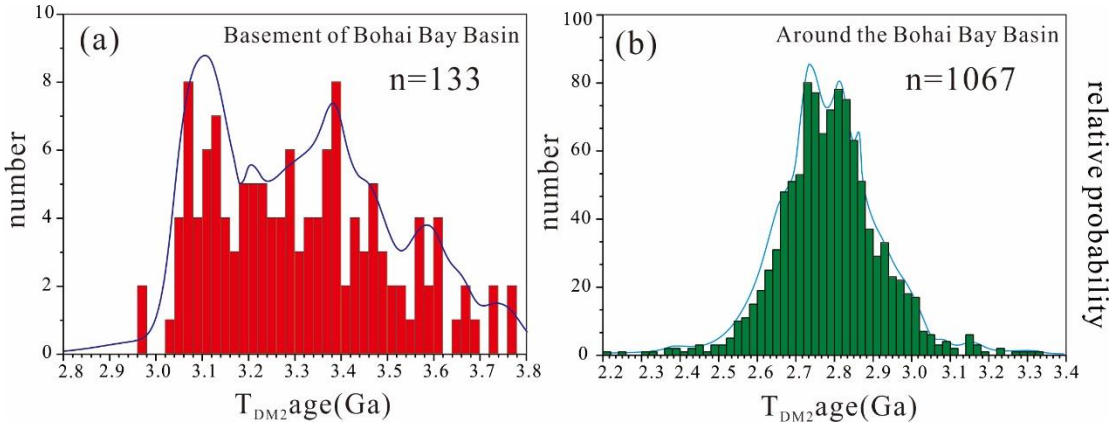

893

894 **Fig.10 Histogram of two-stage Hf model ages with the U-Pb age of 2.6-2.5Ga**

895 (a) Archean basement of the Jiyang depression of the Bohai Bay Basin; (b) Archean basement around
896 the Bohai Bay Basin

897 Data source for Archean basement of around the Bohai Bay Basin: Wu et al., 2008; Yang et al., 2008; Li
898 et al., 2010; Wan et al., 2011; Wang et al., 2011b; Lv et al., 2012; Peng et al., 2012a; Wang et al., 2012;
899 Liu et al., 2013; Meng et al., 2013; Wang et al., 2013; Wu et al., 2013; Wan et al., 2014b; Guo et al.,
900 2015; Wu et al., 2016; Sun et al., 2020

901

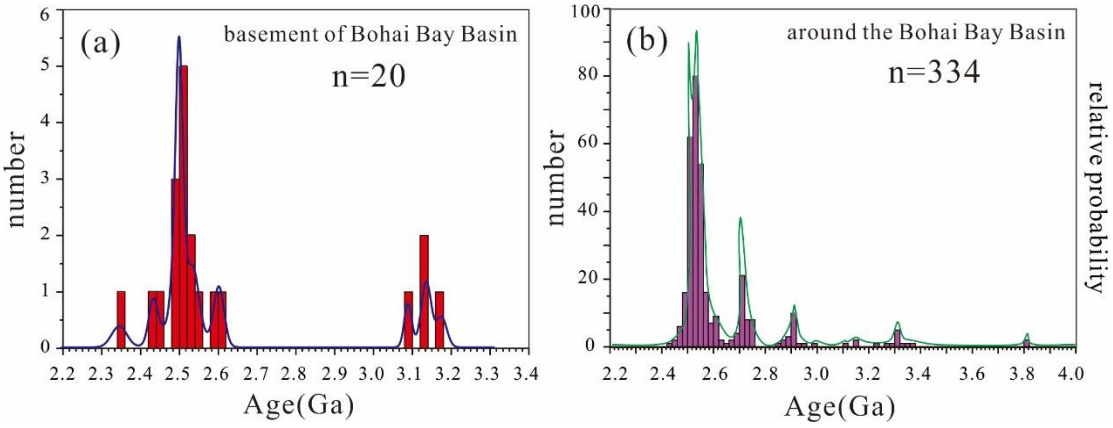

902

903

904

905 **Fig.11 Age histogram of of magmatic zircons.**

906 (a) Basement of Bohai Bay Basin (this study and Song et al.,2011; Wan et al., 2014a; Wang et al.,2019)
907 (b) Around the Bohai Bay Basin (Liu et al., 1990; Kröner et al., 1998; Li and Shen, 2000; Du et al., 2003;
908 Lu et al., 2004; Wan et al., 2005; Geng et al., 2006; Shen et al., 2007; Tang et al., 2007; Jahn et al., 2008;
909 Liu et al., 2008; Lu et al., 2008; Wang et al., 2008; Wu et al., 2008; Yang et al., 2008; Zhao et al., 2008;
910 Grant et al., 2009; Li et al., 2010; Wan et al., 2010; Liu et al., 2011; Nutman et al., 2011; Wan et al.,
911 2011; Lv et al.,2012; Peng et al., 2012b; Wan et al., 2012b; Guo et al., 2013; Meng et al., 2013; Wan et
912 al., 2013; Wang et al., 2013; Wu et al., 2013; Wu et al., 2014; Xie et al., 2014; Guo et al., 2015; Wang
913 et al., 2015; Bai et al., 2016; Sun et al., 2020)

914